

The Influence of Molecular Geometry on the Efficiency of Thermally Activated Delayed Fluorescence.

Roberto S. Nobuyasu,^{1‡} Jonathan S. Ward,^{2‡} Jamie Gibson,³ Beth A. Laidlaw,³ Zhongjie Ren,^{2,4} Przemyslaw Data,¹ Andrei S. Batsanov,² Thomas J. Penfold,^{3*} Martin R. Bryce,^{2*} and Fernando B. Dias.^{1*}

¹Durham University, Physics Department, South Road, Durham, DH1 3LE, UK.

²Durham University, Chemistry Department, South Road, Durham, DH1 3LE, UK.

³Chemistry-School of Natural and Environmental Sciences, Newcastle University, Newcastle upon Tyne, NE1 7RU, UK.

⁴Beijing University of Chemical Technology, State Key Laboratory of Chemical Resource Engineering, Beijing 100029 China

‡ These authors contributed equally to this work.

* email of corresponding authors:

f.m.b.dias@durham.ac.uk, tom.penfold@ncl.ac.uk, m.r.bryce@durham.ac.uk

Supporting Information

S1. Electrochemistry.

The ionization potential (IP) and electron affinity (EA) were determined from the onset of the redox peaks, assuming the potentials are expressed on the absolute potential scale, i.e. with respect to the vacuum level. The absolute potential of Fc/Fc⁺ in non-aqueous electrolytes is 5.1 V.^[S1-S3] This leads to the following equations:

$$\text{IP(eV)} = |e|(E_{\text{ox(onset)}} + 5.1) \quad (1)$$

$$\text{EA(eV)} = -|e|(E_{\text{red(onset)}} + 5.1) \quad (2)$$

The energies associated with the HOMO and LUMO orbitals were estimated from the EA and IP potentials,^[S3, S4] using an electrochemical cell containing a platinum electrode with 1 mm diameter of working area as the working electrode, an Ag/AgCl electrode as the reference electrode, and a platinum coil as an auxiliary electrode. Cyclic voltammetry measurements were conducted at room temperature at a scan rate of 50 mV/s, calibrated against a ferrocene/ferrocenium redox couple. Solvents were dried before use, and electrochemical measurements were conducted in 1.0 mM concentrations of all compounds. Electrochemical studies were undertaken in 0.1 M solutions of Bu₄NBF₄, 99% (Sigma Aldrich) in dichloromethane (DCM), THF or DMF solvent, CHROMASOLV[®], 99.9% (Sigma Aldrich) at room temperature. Although, the presented CVs were recorded in dichloromethane based electrolyte, additional checks were performed in THF and DMF for the reductions. No significant change in the potential was observed and therefore the data presented can be deemed to be reliable.

All of the investigated compounds were electroactive and showed both oxidation and reduction processes (Figure S1.1). The larger change in the IP energy is observed with increasing the size of the alkyl group (compounds **1-4**, from -5.4 \rightarrow -6.1 eV) (Figures S1.1a, and S1.2). This is consistent with the alkyl group inducing changes in conformation of the phenothiazine. Interestingly, there is almost no difference in energy of the IP and EA potentials between *t*-butyl mono-substitution and methyl bi-substitution (Figure S1.2, compounds **4** and **5**).

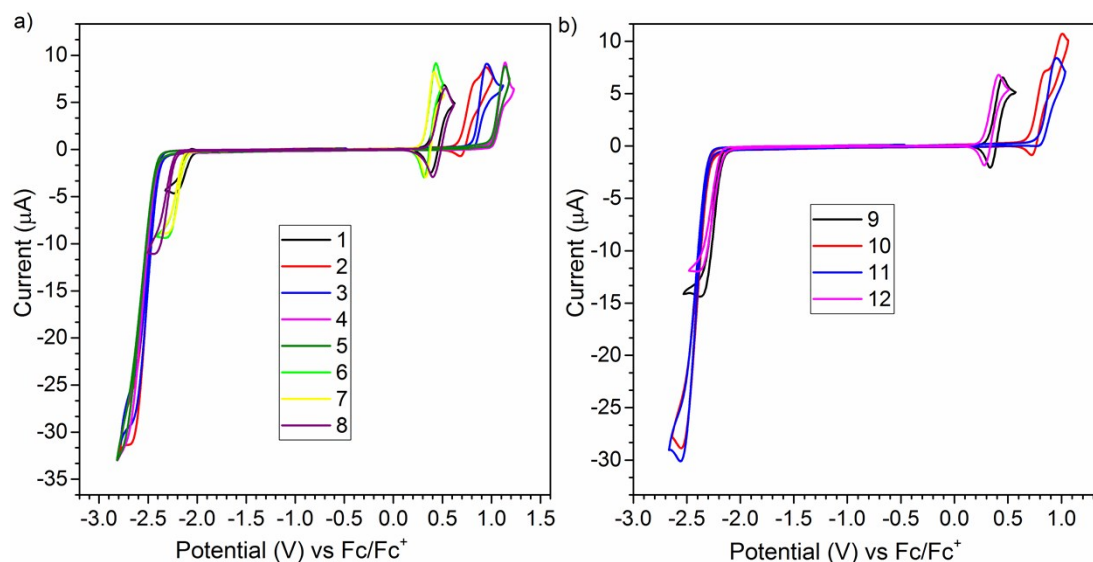


Figure S1.1 - Cyclic voltammetry of 2 mM concentration of investigated compounds in 0.1M Bu₄NBF₄/DCM. Measurement conditions: scan rate 50 mV/s, Ag/AgCl – quasi-reference electrode, calibrated against a ferrocene/ferrocenium redox couple.

When the alkyl group was connected to acceptor instead of the donor unit there almost no change in the IP energy is observed. However, there is a small change in the EA energy. In our present work the substituents are systematically increased in steric bulk at the same position on the donor. It is expected that the electron donating strength in the present series of compounds will not vary significantly as the difference in inductive effects of Me, *i*Pr, *t*Bu are subtle and minor. It is likely that both effects (bulk and electron-donating ability) are contributing simultaneously and it is not possible to decouple the two effects. Indeed, it would be very difficult to design a molecule where steric bulk is introduced without simultaneously introducing a minor change in electronic effects. However, evidence supporting a more dominant role of steric effects is revealed by control molecule **12**, which has a Me substituent in a remote position. The IP value of **12** is very similar to unsubstituted **9** (Figure S1.2) whereas **10** and **11** have a significantly increased IP compared to **9**. A similar steric effect is observed with bulky substituents in **2-4**, relative to **1**.

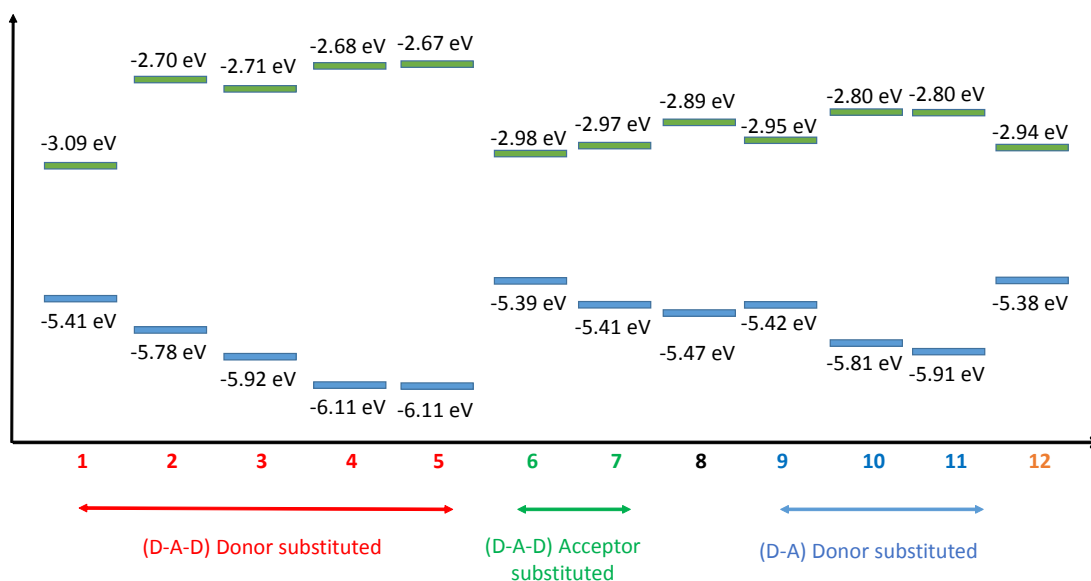


Figure S1.2 - Evolution of the IP and EA potentials with substitution on the donor and acceptor units for all molecules discussed.

S2. Computational Studies.

Computational Details. The ground and excited S_1 state geometries were optimized using density functional theory (DFT) or time-dependent DFT (TDDFT) within the approximation of the M062X exchange and correlation functional^[S5] and a Def2SVP basis^[S6] as implemented within the Gaussian 09 quantum chemistry package.^[S7] The ground state geometries were used to simulate the absorption spectra, and solvent effects were included using a Polarizable Continuum Model (PCM) with the dielectric constant for dichloromethane (DCM).^[S8] The S_1 geometries were used to calculate the emission energies, and here the effect of solvation was incorporated using the state-specific polarizable continuum solvation model (SS-PCM).^[S8] For molecules with more than one major conformer the absorption spectra were obtained by linear combination of the spectrum calculated for each conformer weighted a Boltzmann factor determined from their respective energies.

S2.1 Calculated Energies for the Different Conformers.

Table S2.1^a - The relative energies, dipole moment (Debye), HOMO and LUMO energies (eV), and Boltzmann distributions of the major conformers for the 8 D-A-D molecules studied herein.

	1			5			8		
Conformer	Ax.	Eq.	M.	Ax.	Eq.	M.	Ax.	Eq.	M.
Rel. Energy (eV)	0.00	0.15	0.07	0.00	0.64	0.33	0.20	0.16	0.00
Dipole (D)	10.73	4.04	9.07	10.70	8.40	10.43	11.05	4.97	9.75
E _{HOMO} (eV)	-7.11	-6.65	-6.64	-7.18	-7.09	-7.09	-6.99	-6.78	-6.80
E _{LUMO} (eV)	-1.02	-1.49	-1.24	-0.99	-1.39	-1.17	-0.86	-1.38	-1.06
Boltzmann Weighting	0.94	0.00	0.06	1.00	0.00	0.00	0.11	0.61	0.28

	2			3			4		
Conformer	Ax.	Eq.	M.	Ax.	Eq.	M.	Ax.	Eq.	M.
Rel. Energy (eV)	0.00			0.00			0.00		
Dipole (D)	10.86			10.83			10.82		
E _{HOMO} (eV)	-7.17			-7.17			-7.31		
E _{LUMO} (eV)	-1.00			-0.99			-0.98		
Boltzmann Weighting	1.00			1.00			1.00		

	6			7		
Conformer	Ax.	Eq.	M.	Ax.	Eq.	M.
Rel. Energy (eV)		0.00			0.00	
Dipole (D)		4.94			4.72	
E _{HOMO} (eV)		-6.66			-6.77	
E _{LUMO} (eV)		-1.36			-1.36	
Boltzmann Weighting		1.00			1.00	

	9		10		11		12	
Conformer	Ax.	Eq.	Ax.	Eq.	Ax.	Eq.	Ax.	Eq.
Rel. Energy (eV)	0.00	0.06	0.00		0.00		0.00	0.08
Dipole (D)	9.33	6.22	9.18		9.38		9.89	6.41
E _{HOMO} (eV)	-7.18	-6.64	-7.26		-7.30		-7.16	-6.56
E _{LUMO} (eV)	-1.09	-1.34	-1.09		-1.08		-1.08	-1.33
Boltzmann Weighting	0.91	0.09	1.00		1.00		0.95	0.05

^a The computational simulations show that a specified conformer is not formed at all in some compounds. This is the case for compounds **2**, **3**, **4**, **10** and **11** where only the axial form is present in the ground state, and for compounds **6** and **7** where only the equatorial form is predicted to exist, also in the ground state. Therefore no data is reported in these cases.

S2.2 Calculated IP and EA potentials.

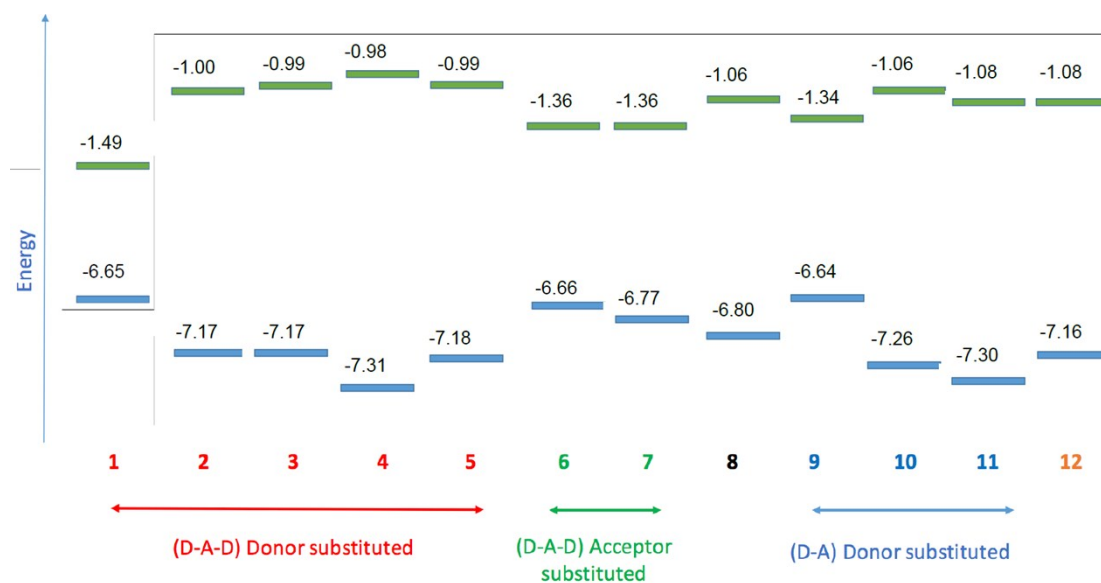


Figure S2.2- The HOMO and LUMO energies (in eV) calculated for the 12 compounds studied in this work. The trend is in excellent agreement with the experimental IP and EA potentials determined experimentally (Figure S2).

S2.3 Calculated Excited State Energies.

Table S2.3^a - Energies (in eV) for the S₁ states and close lying triplet states, for the D–A–D and D–A conformers at the excited state equilibrium geometry (S₁). The bottom row is the energy gap (in eV) between the S₁ and the triplet state of the same character, which in all cases is the T₁. The solvent included in the SS-PCM formalism is toluene.

Conformer	1			5			8		
	Ax.	Eq.	M.	Ax.	Eq.	M.	Ax.	Eq.	M.
T ₁	2.78	1.91	2.15	2.79	2.66	2.80	2.57	-	2.51
T ₂	3.28	-	-	3.39	3.21	-	-	-	-
T ₃	-	-	-	3.78	3.57	-	-	-	-
S ₁ (<i>f</i>)	3.68 (0.0038)	1.93 (0.0002)	2.18 (0.0004)	3.79 (0.0078)	3.73 (0.0004)	2.92 (0.0008)	3.58 (0.0158)	-	2.95 (0.0116)
ΔE _{S1-Tn}	0.90	0.02	0.03	1.0	0.07	0.12	1.01	-	0.44

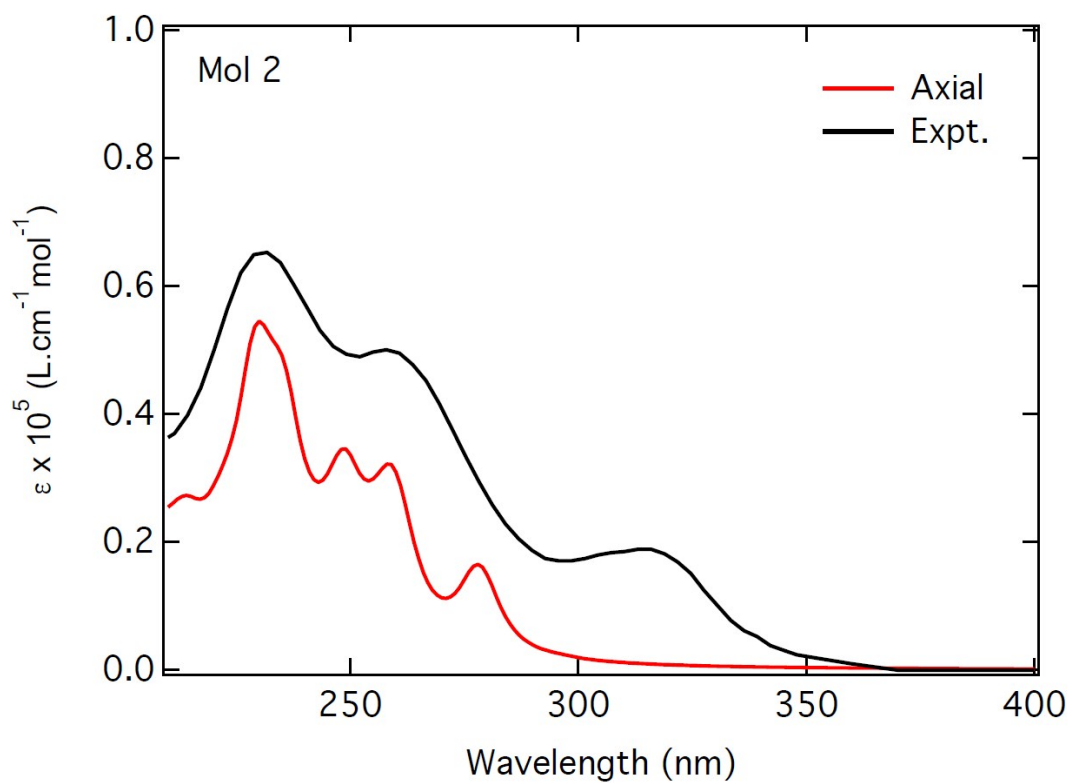
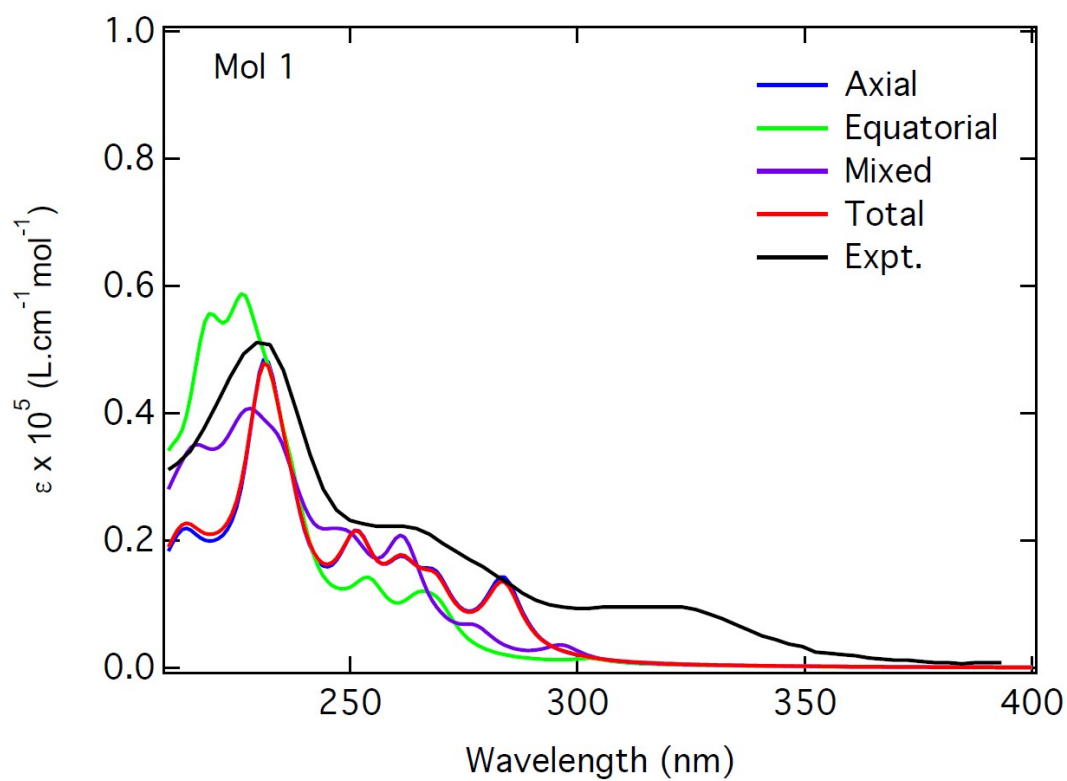
Conformer	2			3			4		
	Ax.	Eq.	M.	Ax.	Eq.	M.	Ax.	Eq.	M.
T ₁	2.78	-	2.26	2.83	-	-	2.79	-	-
T ₂	3.34	-	-	3.38	-	-	3.45	-	-
T ₃	-	-	-	3.77	-	-	3.78	-	-
S ₁ (<i>f</i>)	3.74 (0.0053)	-	2.34 (0.0109)	3.79 (0.0019)	-	-	3.84 (0.0250)	-	-
ΔE _{S1-Tn}	0.94	-	0.08	0.96	-	-	1.05	-	-

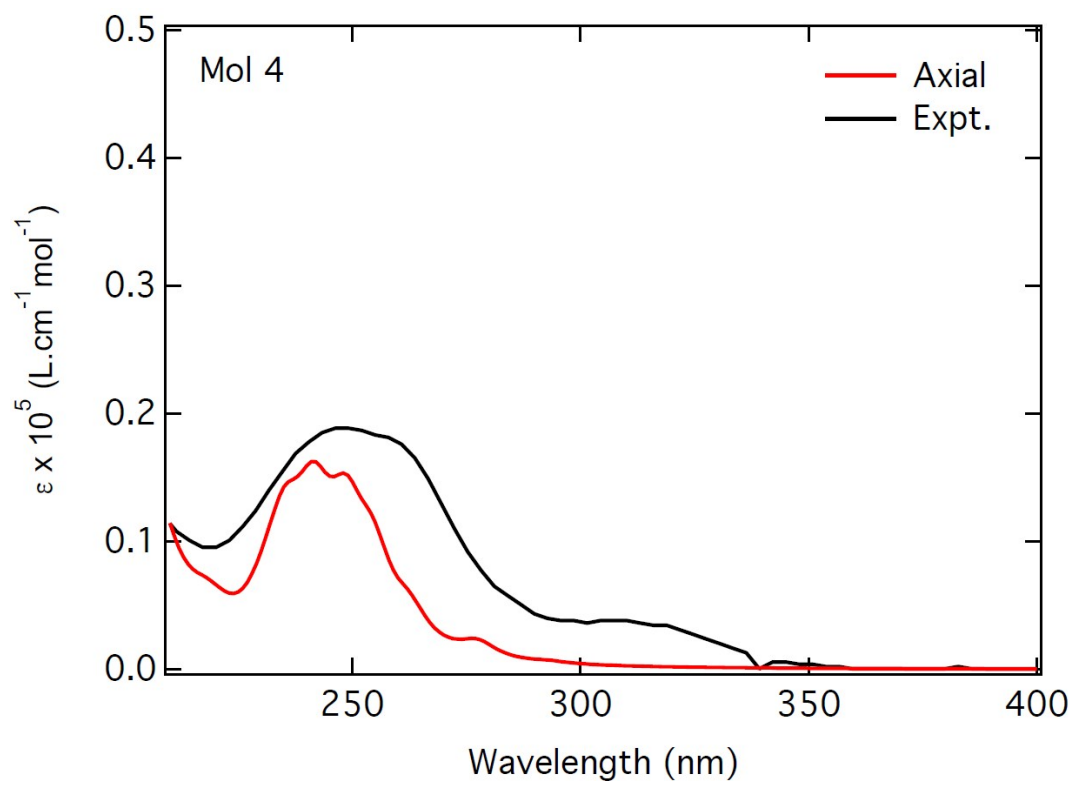
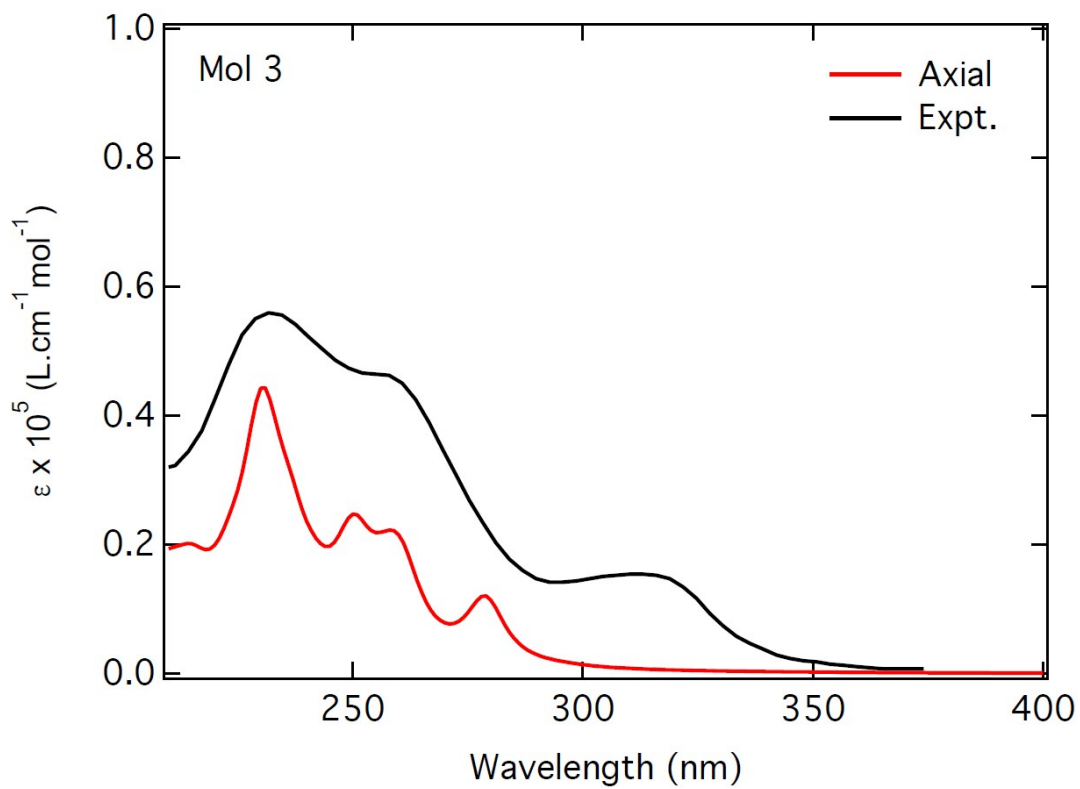
Conformer	6			7		
	Ax.	Eq.	M.	Ax.	Eq.	M.
T ₁	-	2.15	-	-	2.22	-
T ₂	-	-	-	-	-	-
T ₃	-	-	-	-	-	-
S ₁ (<i>f</i>)	-	2.16 (0.0002)	-	-	2.23 (0.0000)	-
ΔE _{S1-Tn}	-	0.01	-	-	0.01	-

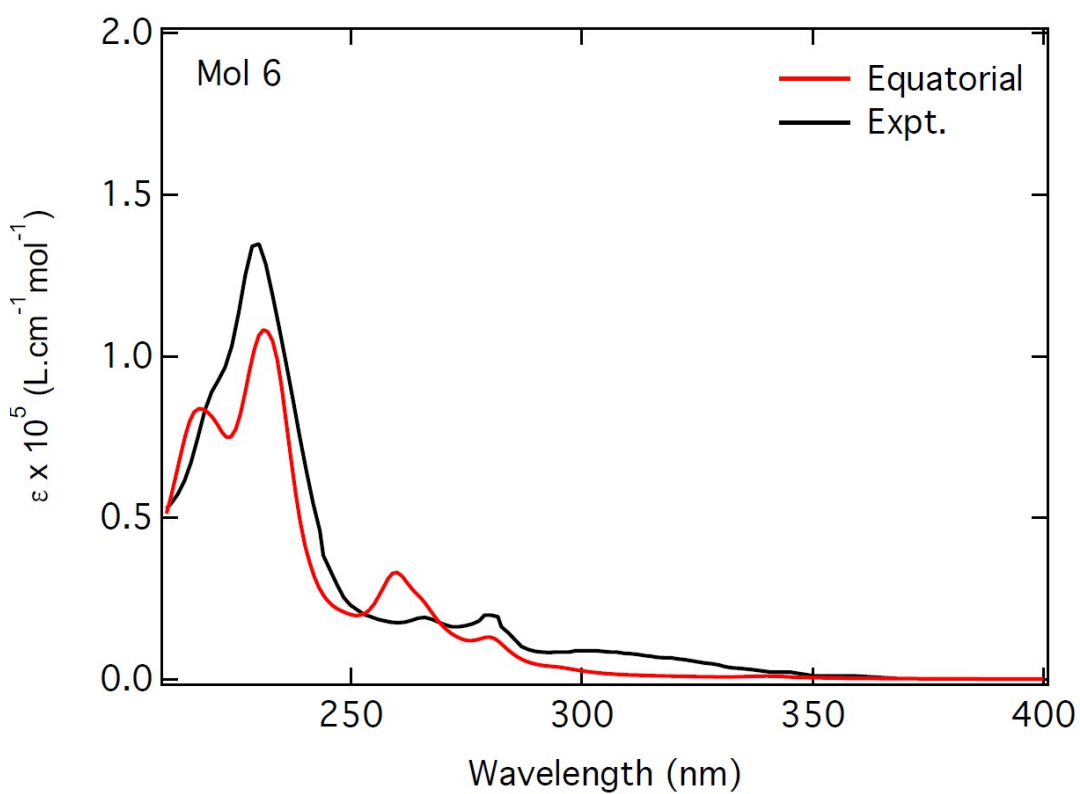
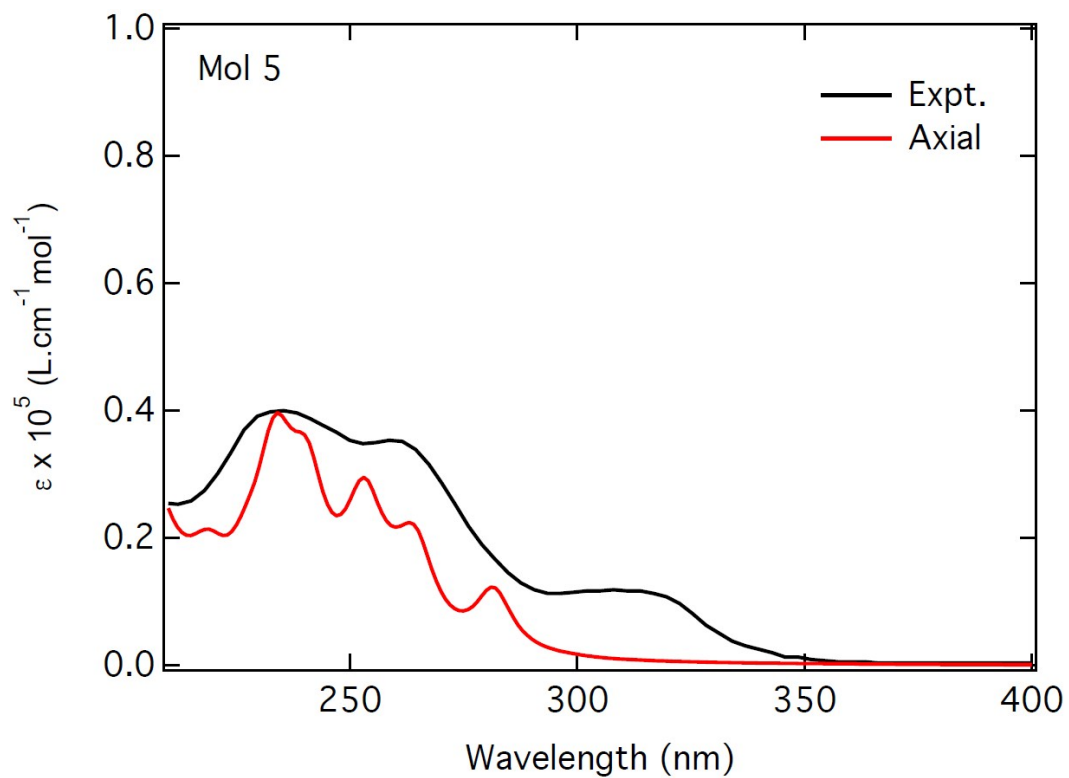
Conformer	9		10		11		12	
	Ax.	Eq.	Ax.	Eq.	Ax.	Eq.	Ax.	Eq.
T ₁	-	1.99	2.78	-	2.33	-	-	1.93
T ₂	-	-	3.50	-	-	-	-	-
T ₃	-	-	-	-	-	-	-	-
S ₁ (<i>f</i>)	-	2.01 (0.0002)	3.66 (0.0684)	-	2.41 (0.0209)	-	-	1.94 (0.0002)
ΔE _{S1-Tn}	-	0.02	0.88	-	0.08	-	-	0.01

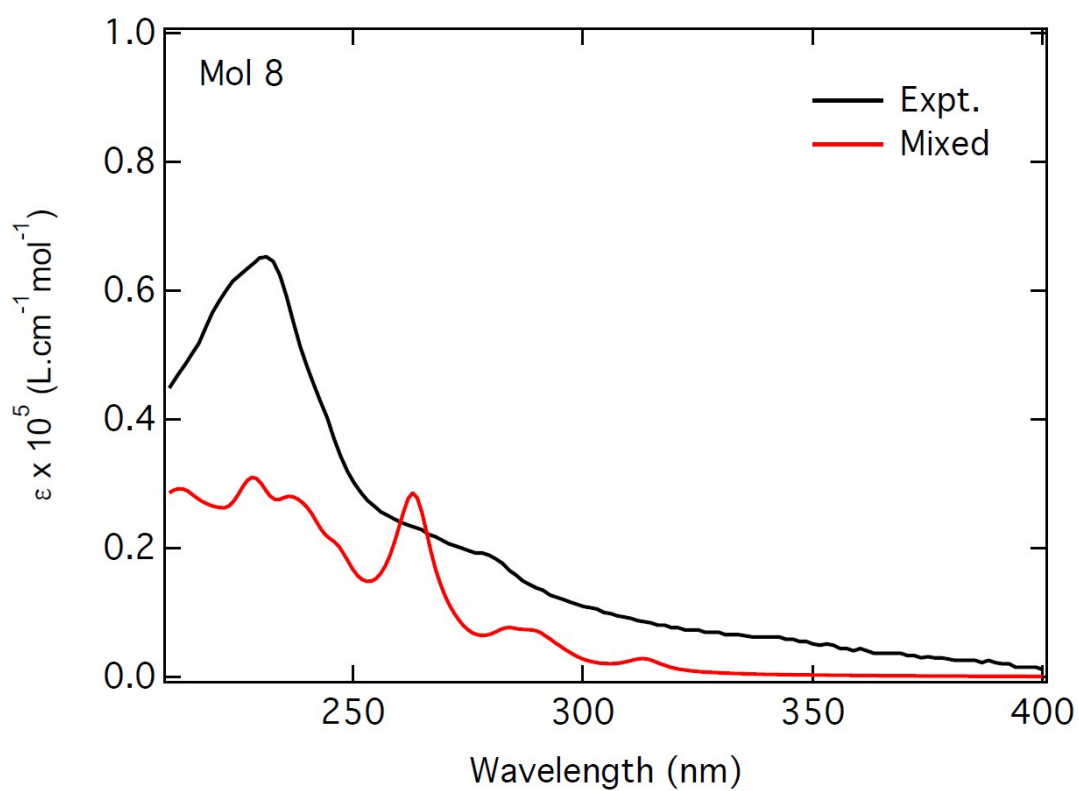
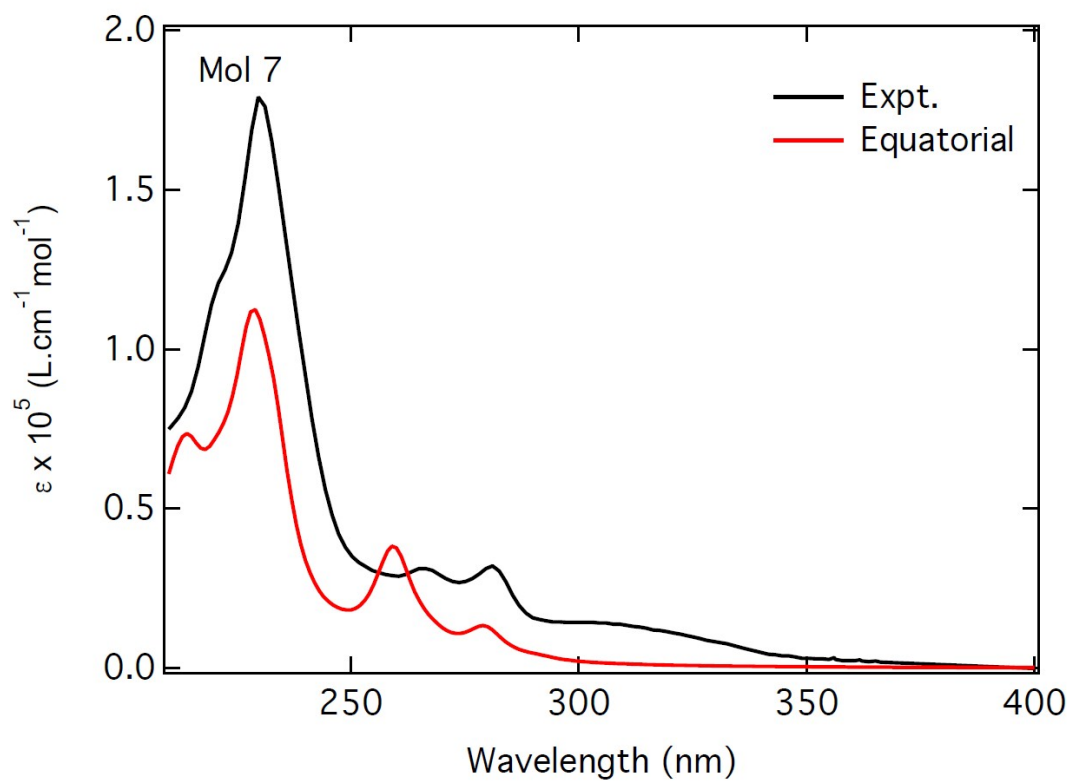
^a The computational simulations show that a specified conformer is not formed at all in the excited state of some compounds. This is the case for compound **8**, that shows contributions from only axial and mixed forms, **2-4**, **10**, and **11** that show only contributions from the axial form, and **6**, **7**, **9** and **12** that show contributions from the equatorial form only. In some cases the calculations were also not able to find higher triplet levels for specified conformers. Therefore no data is reported in these cases.

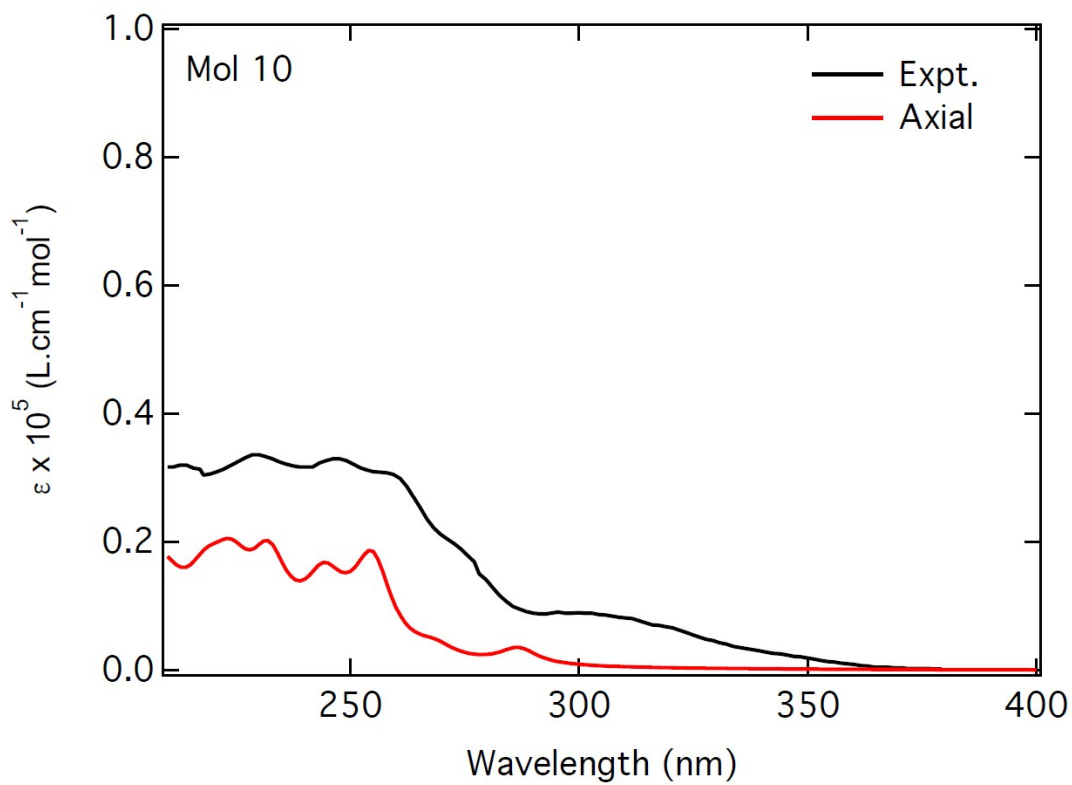
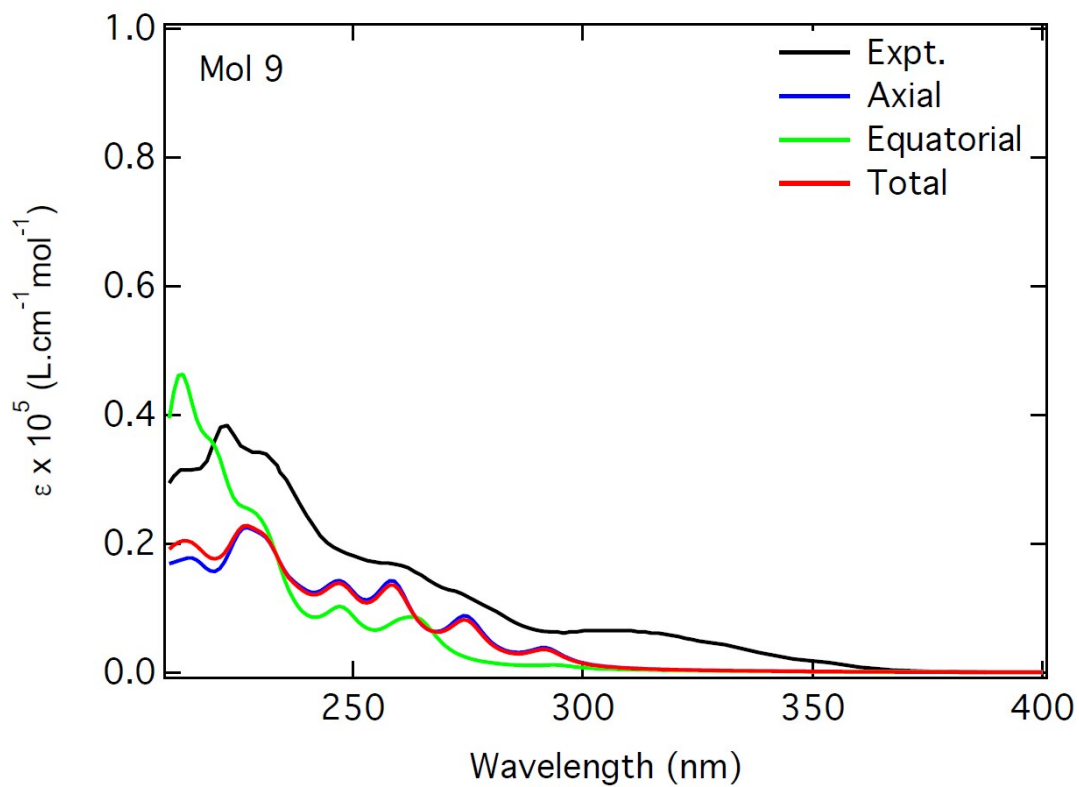
S2.4 Calculated Absorption Spectra of compounds 1-12.

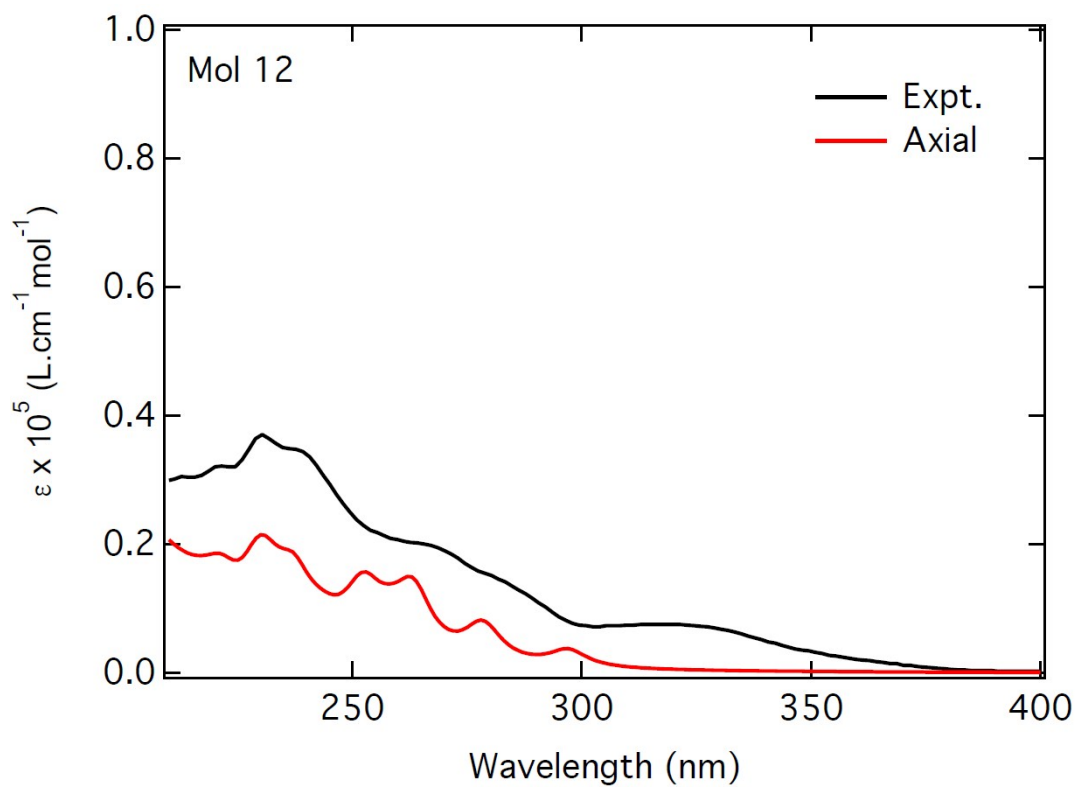
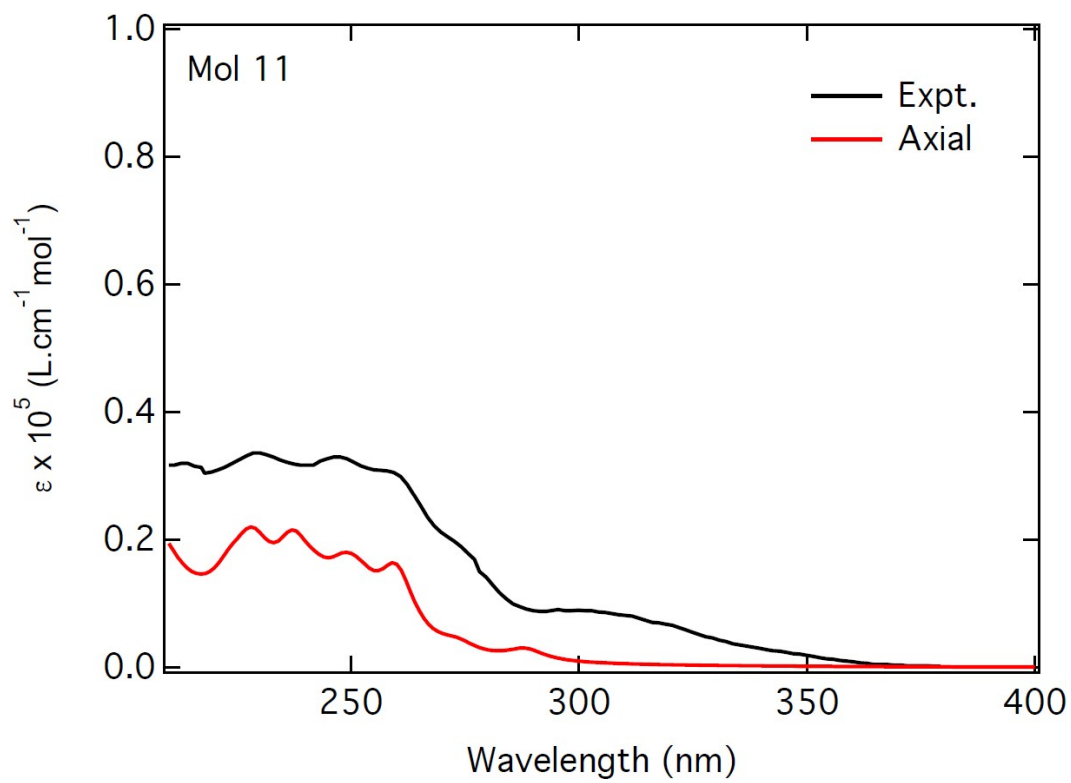












S3. X-Ray Crystallography

X-ray diffraction experiments (**Table S3.1**) were carried out on a Bruker 3-circle D8 Venture diffractometer with a PHOTON 100 CMOS area detector, using Mo- K_{α} (**6**, **7**) or Cu- K_{α} (**8**) radiation from Incoatec I μ S microsources with focussing mirrors. Crystals were cooled using a Cryostream (Oxford Cryosystems) open-flow N₂ gas cryostat. The data were processed using APEX3 v.2016.1-0 and reflection intensities integrated using SAINT v8.38A software (Bruker AXS, 2016). **8**·CDCl₃ was studied at Beamline I19 of Diamond Light Source (RAL) on a dual air-bearing fixed- χ diffractometer with pixel-array photon-counting Dectris Pilatus 2M detector,^[S9] using undulator radiation monochromated with double-crystal Si(111). The crystal was cryo-mounted using a remote-controlled BART robot^[S10] and cooled using a Cryostream N₂ gas cryostat. The diffraction images were converted to Bruker format using `cbf_to_sfrm.py` program^[S11] and further processed with APEX3 and SAINT software (*vide supra*). The data were corrected for absorption by a semi-empirical method based on Laue equivalents and multiple scans, using SADABS program,^[S12] except that of **8** (a 2-component non-merohedral crystal twinned by a 180° rotation around the *z* axis), which was scaled using TWINABS 2012/1 program (Bruker AXS, 2008-2012). Structure **6** was solved by iterative method using `olex2.solve` program,^[S13] **7** by direct methods using SHELXS 2013/1 program,^[S14] **8** and **8**·CDCl₃ by dual-space intrinsic phasing method using SHELXT 2018/2 program^[S15], and refined by full-matrix least squares using SHELXL software^[S16] on OLEX2 platform.^[S17]

On cooling below 180 K, compound **7** undergoes a gradual and reversible phase transition with doubling of the *c* parameter. The structures were determined at 190 K (RT-phase) and 120 K (LT-phase). The latter has a sublattice (corresponding to the actual lattice of the RT-phase) and contains two independent molecules of nearly the same conformations as the single one in the RT-phase.

Table S3.1. Crystal data and experimental details

Compound	6	7 (high T)	7 (low T)	8	8 ·CDCl ₃
CCDC no.	1884010	1884007	1884011	1884008	1884009
Formula	C ₃₈ H ₂₆ N ₂ O ₂ S ₃	C ₄₂ H ₃₄ N ₂ O ₂ S ₃	C ₄₂ H ₃₄ N ₂ O ₂ S ₃	C ₄₄ H ₃₈ N ₂ O ₂ S ₃	C ₄₄ H ₃₈ N ₂ O ₂ S ₃ ·CDCl ₃
Formula weight	638.79	694.89	694.89	722.94	843.32
$D_{calc.}/g\text{ cm}^{-3}$	1.441	1.360	1.375	1.325	1.396
μ/mm^{-1}	0.29	0.26	0.26	2.19	0.39
T/K	120	190	120	120	100
Radiation	Mo- K_{α}	Mo- K_{α}	Mo- K_{α}	Cu- K_{α}	synchrotron
$\lambda/\text{\AA}$	0.71073	0.71073	0.71073	1.54184	0.6889
Crystal System	triclinic	triclinic	triclinic	monoclinic	monoclinic
Space Group	$P\bar{1}$ (no. 2)	$P\bar{1}$ (no. 2)	$P\bar{1}$ (no. 2)	$C2/c$ (no. 15)	$P2_1/m$ (no. 11)
$a/\text{\AA}$	8.7268(8)	12.9638(8)	12.9513(10)	16.766(4)	7.6155(19)
$b/\text{\AA}$	13.2586(11)	14.1725(10)	14.1812(11)	7.690(2)	31.336(8)
$c/\text{\AA}$	13.8335(12)	9.5622(6)	18.9798(15)	28.118(7)	8.892(2)
$\alpha/^\circ$	79.822(3)	77.138(2)	76.632(3)	90	90
$\beta/^\circ$	75.146(3)	84.451(2)	83.723(3)	90.899(4)	108.991(5)
$\gamma/^\circ$	73.305(3)	83.336(3)	83.531(3)	90	90
$V/\text{\AA}^3$	1472.7(2)	1696.65(19)	3357.3(5)	3625.0(16)	2006.4(9)
Z	2	2	4	4	2
$2\theta_{max}/^\circ$	50	50.25	50	151.1	50
Reflections total	23441	23900	53040	18203	20383
unique	5185	6043	11804	3518	3922
with $I > 2(I)$	3435	3903	8686	3035	3441
R_{int}	0.086	0.064	0.047	0.060	0.089
Parameters/restraints	409/0	451/6	899/0	253	327/271
$\Delta\rho_{max, min}/e\text{\AA}^{-3}$	0.33, -0.31	0.40, -0.34	0.44, -0.40	0.31, -0.33	0.70, -1.06
Goodness of fit	1.014	1.105	1.028	1.062	1.025
R_1, wR_2 (all data)	0.093, 0.098	0.095, 0.113	0.069, 0.121	0.063, 0.107	0.106, 0.270
$R_1, wR_2 [I > 2(I)]$	0.046, 0.084	0.049, 0.095	0.043, 0.108	0.049, 0.099	0.099, 0.263

Table S3.2. Molecular geometry of **6-8**

	$\tau_1 / ^\circ$	$\theta_1 / ^\circ$	$\tau_2 / ^\circ$	$\theta_2 / ^\circ$	C(A)- N/ \AA	C(D)- N/ \AA
6	66.1	151.3	86.6	156.5	1.420(3)	1.436(6)
7 (190 K)	73.0	150.0	87.4	155.3	1.420(5)	1.444(3)
7 (120 K)	70.6	148.0	86.4	155.1	1.422(4)	1.440(3)
	74.0	151.6	87.8	154.6	--	--
8	58.2 ^a	140.4 _a	80.9 ^b	144.0 _b	1.43(1) ^a	1.441(3) _a
8 ·CDCl ₃	67.7 ^a	149.0 _a	74.7 ^b	158.4 _b	1.425(8)	1.430(5)

^a Major isomer; ^b minor isomer

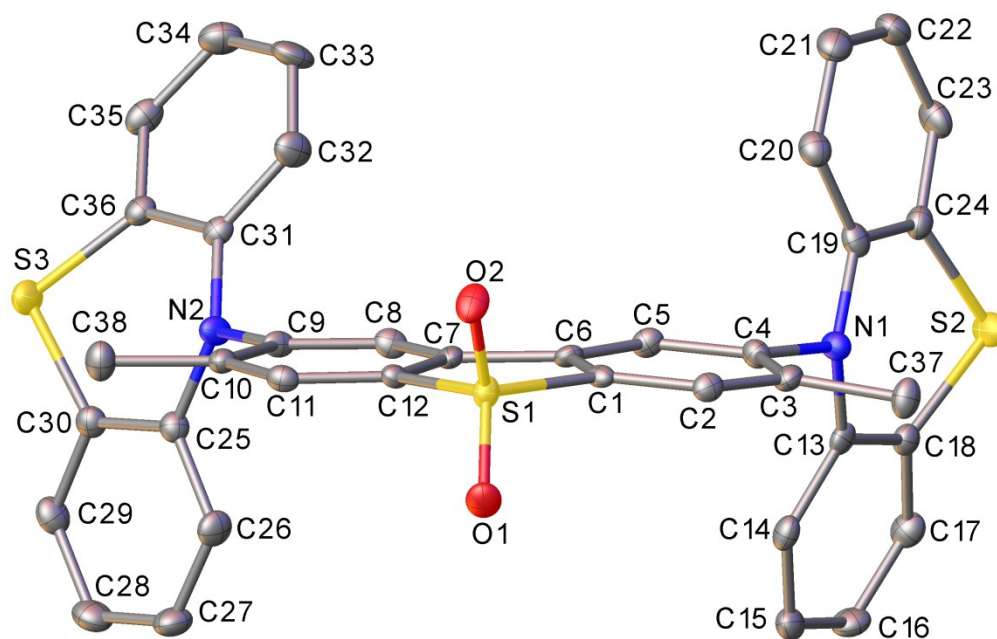
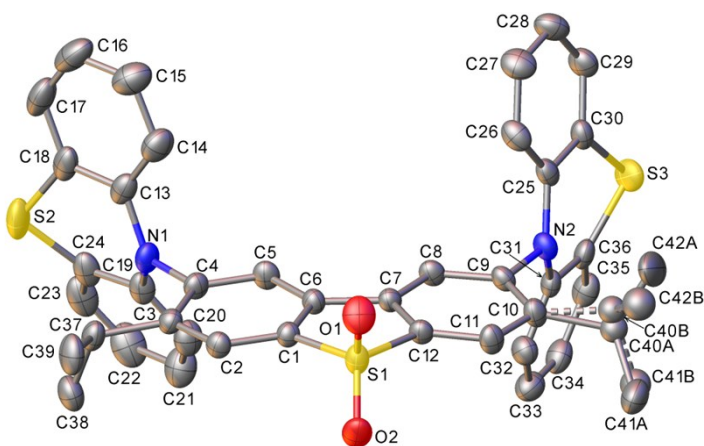


Figure S3.1. X-ray molecular structure of **6**. Thermal ellipsoids are drawn at 50% probability level, H atoms are omitted.



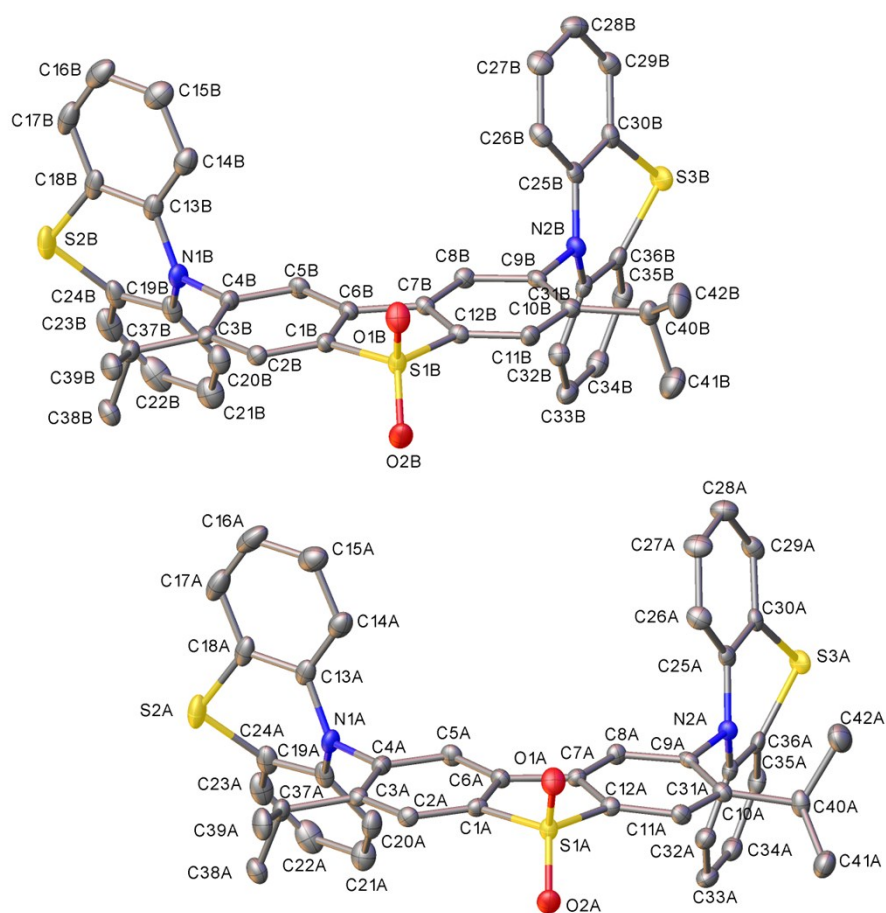


Figure S3.2. X-ray molecular structure of **7** at 190 K (top) and 120 K (bottom, two independent molecules). Thermal ellipsoids are drawn at 50% probability level, H atoms are omitted.

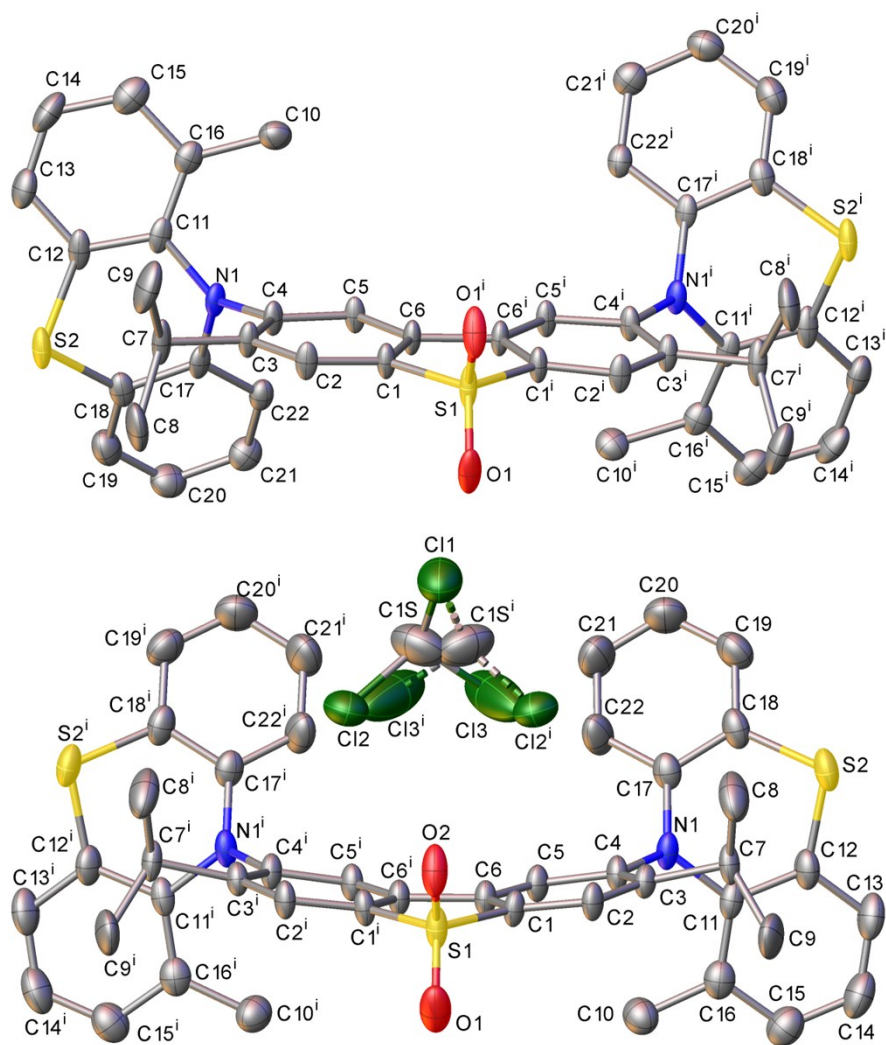


Figure S3.3. X-ray molecular structures of **8** (unsolvated form) (top) and **8**·CDCl₃ (bottom) The primed atoms are generated by twofold axis and mirror plane, respectively. Thermal ellipsoids are drawn at 50% probability level, H atoms and minor conformers are omitted.

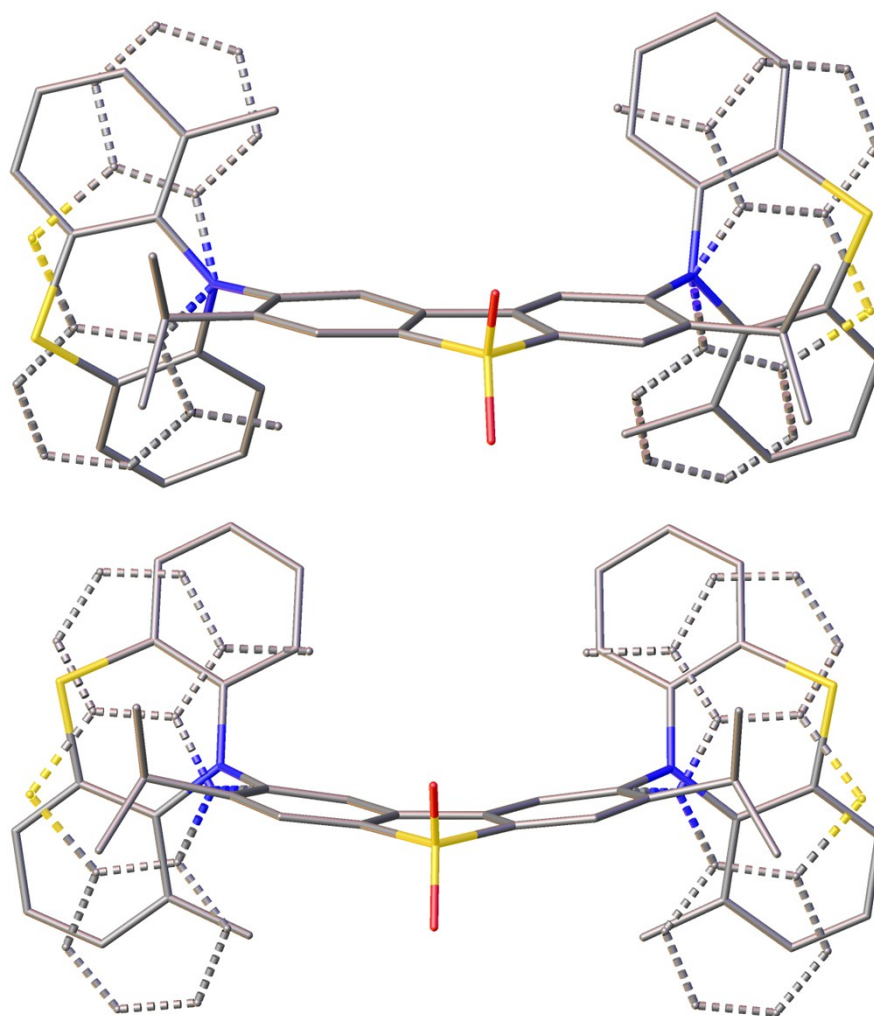


Figure S3.4. Disorder in the crystals of **8** (top) and **8**·CDCl₃; minor conformer is shown dashed.

S4. General chemistry experimental details

All reactions were carried out under an argon atmosphere unless otherwise stated. Starting materials were purchased commercially and were used as received. Solvents were dried using an Innovative Technology solvent purification system and were stored in ampoules under argon.

TLC analysis was carried out using Merck Silica gel 60 F₂₅₄ TLC plates and spots were visualised using a TLC lamp emitting at 365 or 254 nm. Silica gel column chromatography was performed using silica gel 60 purchased from Sigma Aldrich.

¹H and ¹³C NMR spectroscopy was carried out on Bruker AV400 and Varian VNMRs 600 and 700 spectrometers. Residual solvent peaks were referenced as described in the literature^[S18], and all NMR data was processed in MestReNova V12.

Melting points were carried out on a Stuart SMP40 machine with a ramping rate of 4 °C min⁻¹. Videos were replayed manually to determine the melting point.

High resolution mass spectrometry was carried out on a Waters LCT Premier XE using ASAP ionisation and TOF detection. Samples were analysed directly as solids. Any mention of Br in MS data refers to ⁷⁹Br isotope.

Elemental analysis was performed on an Exeter Analytical E-440 machine.

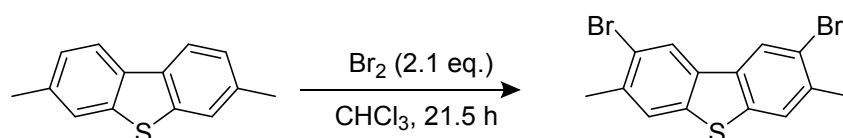
3,7-dimethyldibenzothiophene was prepared according to a literature procedure.^[S19]

2-bromodibenzothiophene-*S,S*-dioxide was prepared according to a literature procedure, using 2-bromodibenzothiophene purchased from TCI chemicals as starting material.^[S20]

Molecules **1**,^[S21] **2–5** and **10–11**,^[S20] and **9**^[S22] were analysed using literature data and samples.

Unless otherwise specified, a mixed isomers grade hexane was used.

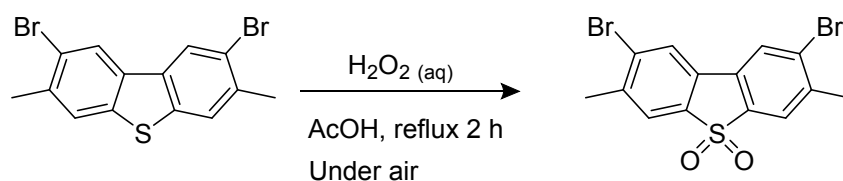
Synthesis of 2,8-dibromo-3,7-dimethyldibenzothiophene



To a dry 50 mL 2-necked round-bottomed flask was added 3,7-dimethyldibenzothiophene (1.00 g, 4.7 mmol, 1 eq.). The solid was dried under vacuum for 30 min and the flask was backfilled with argon. Dry chloroform (20 mL) was added, and the mixture was stirred to allow dissolution. The reaction was cooled to 0 °C and bromine (1.56 g/ 500 μL, 9.8 mmol, 2.1 eq.) was added dropwise. The reaction mixture was allowed to warm to room temperature and was stirred for 21 h. The precipitate that formed was filtered and washed with cold *n*-hexane to give product as a white solid (1.40 g, 80% yield)

¹H NMR (400 MHz, CDCl₃) δ 8.21 (s, 2H), 7.66 (s, 2H), 2.53 (s, 6H); ¹³C{¹H} NMR (176 MHz, CDCl₃) δ 138.9, 136.7, 134.2, 125.1, 124.2, 121.7, 23.6. HRMS-ASAP-TOF⁺ *m/z* calculated for C₁₄H₁₀SBr₂ [M]⁺ 367.8869, found: 367.8836; Anal. Calc. for C₁₄H₁₀SBr₂ C, 45.43; H, 2.72; N, 0.0 Found: C, 45.34; H, 2.71; N, 0.0; m.p. 226 – 228 °C.

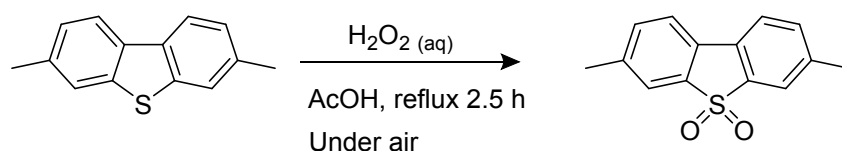
2,8-dibromo-3,7-dimethyldibenzothiophene-*S,S*-dioxide



To a 250 mL round-bottomed flask equipped with a magnetic stirrer bar was added 2,8-dibromo-3,7-dimethyldibenzothiophene (1.00 g, 2.7 mmol, 1 eq.) and acetic acid (40 mL). The mixture was heated with stirring at 80 °C for 30 min to aid dissolution. H₂O_{2(aq)} (12 mL, 35% w/w) was then added to the mixture and was heated to 120 °C for 2 h. The reaction was allowed to cool to ambient temperature, and the precipitate was collected by filtration. The powder was washed with water (4 × 50 mL) with mixing in the sinter. The product was dried at 70 °C overnight, and was purified by silica gel column chromatography eluting with CHCl₃. The product was isolated as a white solid (560 mg, 54% yield).

¹H NMR (400 MHz, CDCl₃) δ 7.91 (s, 2H), 7.66 (s, 2H), 2.51 (s, 6H); ¹³C{¹H} NMR (176 MHz, CDCl₃) δ 141.3, 137.0, 131.2, 129.9, 125.6, 124.0, 23.5; HRMS-ASAP-TOF⁺ *m/z* calculated for C₁₄H₁₀SBr₂O₂ [M]⁺ 399.8768, found: 399.8757; Anal. Calc. for C₁₄H₁₀SBr₂O₂ C, 41.82; H, 2.51; N, 0.0 Found: C, 41.97; H, 2.53; N, 0.0; m.p decomp. > 350 °C.

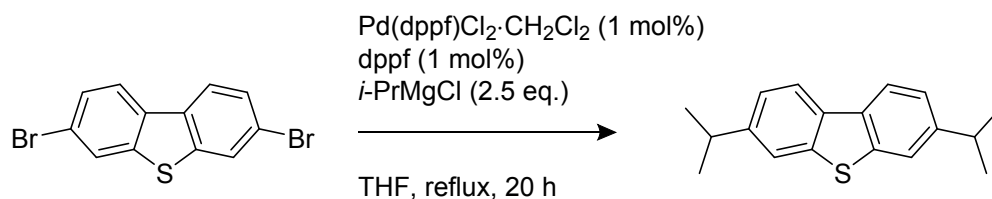
3,7-dimethyldibenzothiophene-*S,S*-dioxide



To a 10 mL round-bottomed flask equipped with a magnetic stirrer bar was added 3,7-dimethyldibenzothiophene (100 mg, 0.47 mmol, 1 eq.) and acetic acid (2 mL). The mixture was heated at 80 °C for 30 min to aid dissolution. H₂O_{2(aq)} (1 mL, 35% w/w) was added and the reaction mixture was heated to 120 °C for 2.5 h. On cooling the mixture down to room temperature a precipitate formed which was collected by filtration, and was washed with water (4 × 10 mL) with mixing in the sinter. The crude product was dried in a 100 °C oven for 2 h and was then dried under vacuum overnight. The crude product was purified by silica gel column chromatography using CH₂Cl₂ as eluent. Removal of solvent under reduced pressure gave product as a white solid. (54 mg, 47% yield).

¹H NMR (400 MHz, DMSO-d₆) δ 8.01 (d, *J* = 8.0 Hz, 2H), 7.77 (s, 2H), 7.58 (d, *J* = 8.0 Hz, 2H), 2.43 (s, 6H); ¹³C{¹H} NMR (101 MHz, DMSO-d₆) δ 140.9, 137.1, 135.0, 128.4, 122.1, 122.0, 20.8; HRMS-ASAP-TOF⁺ *m/z* calculated for C₁₄H₁₃SO₂ [M+H]⁺ 245.0636, found: 245.0639.

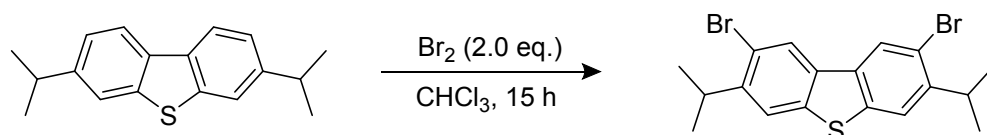
3,7-diisopropyldibenzothiophene



To a 500 mL two-necked round bottomed flask equipped with a stirrer bar and reflux condenser was added 3,7-dibromodibenzothiophene (3.45 g, 10.08 mmol, 1 eq.), Pd(dppf)Cl₂·CH₂Cl₂ (0.082 g, 0.101 mmol, 0.01 eq.) and dppf (0.056 g, 0.101 mmol, 0.01 eq.). The contents were dried under vacuum for 30 min, and the flask was back-filled with argon. Dry THF (200 mL) was then added *via* cannula transfer, and the mixture was deoxygenated with argon bubbling for 30 min. *i*-PrMgCl (2 M in THF, 12.6 mL, 2.5 eq.) was then added *via* syringe, and the reaction was refluxed for 20 h. The reaction was allowed to cool to ambient temperature, and H₂O (100 mL) was added. The organic layer was separated and the aqueous layer was extracted with CH₂Cl₂ (3 × 100 mL). The organic layers were combined and dried with magnesium sulfate and were filtered. Removal of solvent under reduced pressure gave crude material which was purified by silica gel column chromatography. The product was eluted with hexane, followed by 10% CH₂Cl₂/hexane (*v/v*) giving the product as a white solid (1.45 g, approx. 54% yield). Note: Product was approx. 90% pure by NMR and was used in the next reaction without further purification. A small pure sample for analytical purposes was obtained by slow evaporation from acetone. Any impurities present were completely removed from the bulk material in the synthesis of 2,8-dibromo-3,7-diisopropyldibenzothiophene-*S,S*-dioxide.

¹H NMR (400 MHz, CDCl₃) δ 8.01 (d, *J* = 8.2 Hz, 2H), 7.68 (d, *J* = 1.6 Hz, 2H), 7.30 (dd, *J* = 8.2, 1.6 Hz, 2H), 3.05 (hept, *J* = 6.9 Hz, 2H), 1.33 (d, *J* = 6.9 Hz, 12H), ¹³C{¹H} NMR (101 MHz, CDCl₃) δ 147.6, 139.7, 133.8, 123.5, 121.2, 120.3, 34.5, 24.3. HRMS-ASAP-TOF⁺ *m/z* calculated for C₁₈H₂₀S [M]⁺ 268.1286, found: 268.1291; Anal. Calc. for C₁₈H₁₈S: C, 80.55; H, 7.51; N, 0.00 Found: C, 80.49; H, 7.49; N, 0.05; m.p. 146 – 148 °C.

2,8-dibromo-3,7-diisopropyldibenzothiophene

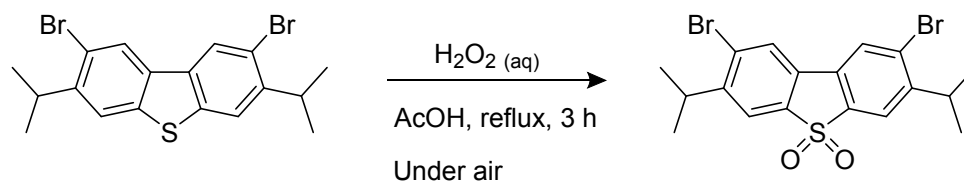


To a dry 50 mL 2-necked round-bottomed flask was added 3,7-diisopropyldibenzothiophene (1.40 g, 5.22 mmol, 1 eq.). The solid was dried under vacuum for 30 min and the flask was backfilled with argon. Dry chloroform (25 mL) was added, and the mixture was stirred to allow dissolution. The reaction was cooled to 0 °C and bromine (1.67 g/ 534 μL, 10.45 mmol, 2.0 eq.) was added dropwise. The

reaction mixture was allowed to warm to room temperature and was stirred for 15 h. Sodium thiosulfate solution (1 M, 20 mL) was added to the reaction mixture, and the mixture was extracted with CH₂Cl₂ (3 × 25 mL). The combined organic layers were dried with magnesium sulfate and were filtered. Removal of solvent under reduced pressure gave crude product. The product was purified by recrystallisation from toluene to give a white solid (1.40 g, 63% yield).

¹H NMR (400 MHz, CDCl₃) δ 8.21 (s, 2H), 7.71 (s, 2H), 3.49 (hept, *J* = 6.9 Hz, 2H), 1.33 (d, *J* = 6.9 Hz, 12H), ¹³C{¹H} NMR (101 MHz, CDCl₃) δ 146.3, 139.5, 134.1, 125.6, 121.2, 120.5, 33.3, 23.2; HRMS-ASAP-TOF⁺ *m/z* calculated for C₁₈H₁₈SBr₂ [M]⁺ 423.9496, found: 423.9498; Anal. Calc. for C₁₈H₁₈SBr₂ C, 50.73; H, 4.26; N, 0.0 Found: C, 50.40; H, 4.19; N, 0.0; m.p. 136 – 138 °C.

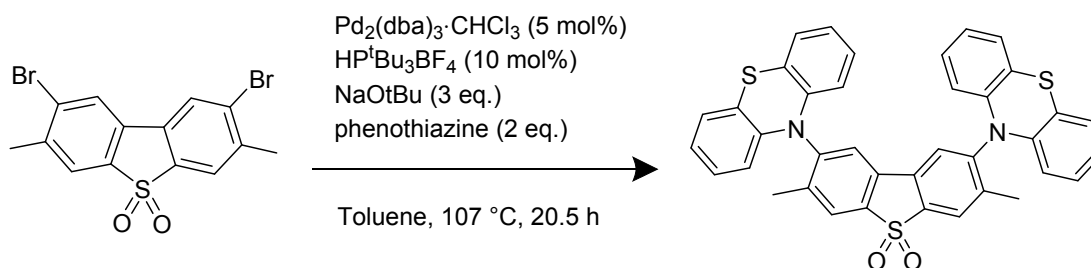
2,8-dibromo-3,7-diisopropyldibenzothiophene-*S,S*-dioxide



To a 250 mL round-bottomed flask equipped with a magnetic stirrer bar was added 2,8-dibromo-3,7-diisopropyldibenzothiophene (1.22 g, 2.86 mmol, 1 eq.) and acetic acid (50 mL). The mixture was heated with stirring at 80 °C for 30 min to aid dissolution. H₂O_{2(aq)} (12 mL, 35% wt.) was added to the mixture and was heated to 120 °C for two hours. Further H₂O_{2(aq)} (4 mL) was added and the reaction was refluxed for one further hour. The reaction was allowed to cool to ambient temperature, and the precipitate was collected by filtration. The powder was washed several times with water with agitation of the suspension in the sinter during each wash. The product was dried at 70 °C for two hours, and was then dried under high vacuum overnight at ambient temperature. The product was isolated as a white solid (1.00 g, 76% yield).

¹H NMR (400 MHz, CDCl₃) δ 7.92 (s, 2H), 7.72 (s, 2H), 3.44 (hept, *J* = 6.8 Hz, 2H), 1.30 (d, *J* = 6.8 Hz, 12H). ¹³C{¹H} NMR (101 MHz, CDCl₃) δ 150.8, 137.5, 130.5, 129.6, 126.1, 120.4, 33.6, 22.6; HRMS-ASAP-TOF⁺ *m/z* calculated for C₁₈H₁₇SBr₂O₂ [M-H]⁺ 454.9316, found: 454.9323, Anal. Calc. for C₁₈H₁₈SBr₂O₂ C, 47.18; H, 3.96; N, 0.0 Found: C, 46.72; H, 3.93; N, 0.0; m.p 245 – 247 °C.

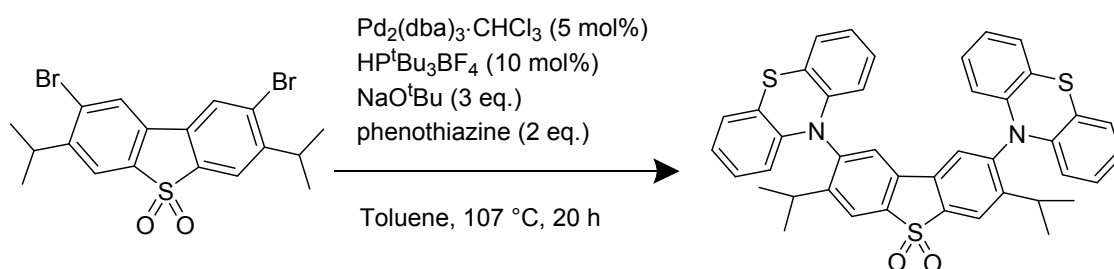
2,8-Bis(phenothiazin-10-yl)-3,7-dimethyldibenzothiophene-*S,S*-dioxide (6)



2,8-dibromo-3,7-dimethyldibenzothiophene-*S,S*-dioxide (156 mg, 0.39 mmol, 1 eq.) and phenothiazine (155 mg, 0.78 mmol, 2 eq.) were dried under vacuum for 30 min in a two-neck 100 mL round-bottomed flask fitted with a reflux condenser. The flask was back-filled with argon and dry toluene (15 mL) was added *via* syringe. The reaction mixture was bubbled with argon for 30 min, then Pd₂(dba)₃·CHCl₃ (20 mg, 19 μmol, 0.05 eq.) and HP^tBu₃BF₄ (11 mg, 38 μmol, 0.1 eq.) was added and the reaction mixture was bubbled with argon for a further 30 min. NaO^tBu (112 mg, 1.17 mmol, 3 eq.) was added under a high flow of argon and the reaction was then heated to 107 °C with stirring for 20.5 h. At the end of the reaction the solvent was removed under reduced pressure and the crude mixture was purified by silica gel column chromatography eluting with 50% *v/v* CH₂Cl₂/hexane switching to 80% CH₂Cl₂/hexane. Removal of solvent under reduced pressure gave product as a yellow solid (198 mg, 80% yield). The product can be sublimed by heating (>350 °C) under high vacuum (9 × 10⁻² mbar). Crystals suitable for X-ray diffraction were obtained by slow evaporation from CD₂Cl₂.

¹H NMR (400 MHz, DMSO-*d*₆) δ 8.45 (s, 2H), 8.29 (s, 2H), 7.05 (dd, *J* = 7.5, 1.6 Hz, 4H), 6.92 (ddd, *J* = 8.2, 7.4, 1.6 Hz, 4H), 6.84 (td, *J* = 7.4, 1.2 Hz, 4H), 6.11 (dd, *J* = 8.2, 1.2 Hz, 4H), 2.27 (s, 6H), ¹³C {¹H} NMR (151 MHz, DMSO-*d*₆) δ 144.2, 142.0, 141.4, 137.0, 131.4, 127.8, 127.0, 126.7, 125.8, 123.0, 118.6, 115.2, 17.5; HRMS-ASAP-TOF⁺ *m/z* calculated for C₃₈H₂₆N₂O₂S₃ [M]⁺ 638.1156, found: 638.1140; Anal. Calc. for C₃₈H₂₆N₂O₂S₃ C, 71.45; H, 4.10; N, 4.39 Found: C, 71.63; H, 4.06; N, 4.41; m.p decomp. > 350 °C.

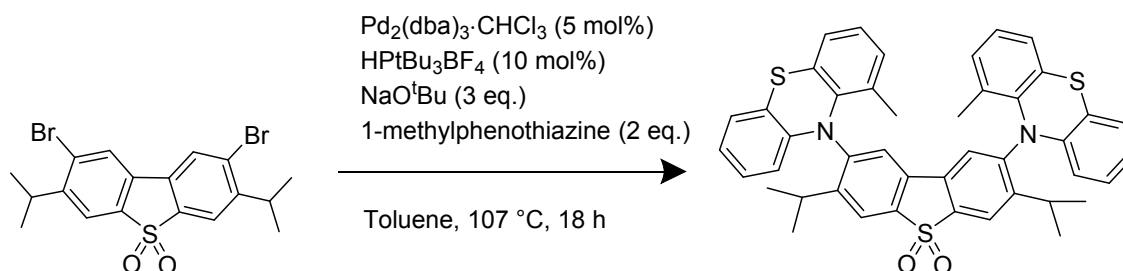
2,8-Bis(phenothiazin-10-yl)-3,7-isopropylidibenzothiophene-*S,S*-dioxide (7)



2,8-dibromo-3,7-diisopropylidibenzothiophene-*S,S*-dioxide (180 mg, 0.39 mmol, 1 eq.) and phenothiazine (156 mg, 0.79 mmol, 2 eq.) were dried under vacuum for 30 min in a two-neck 100 mL round-bottomed flask fitted with a reflux condenser. The flask was back-filled with argon and dry toluene (10 mL) was added *via* syringe. The reaction mixture was bubbled with argon for 30 min, then Pd₂(dba)₃·CHCl₃ (20 mg, 19 μmol, 0.05 eq.) and HP^tBu₃BF₄ (11 mg, 38 μmol, 0.1 eq.) was added and the reaction mixture was bubbled with argon for a further 30 min. NaO^tBu (112 mg, 1.17 mmol, 3 eq.) was added under a high flow of argon and the reaction was then heated to 107 °C with stirring for 20 h. At the end of the reaction the solvent was removed under reduced pressure and the crude mixture was purified by silica gel column chromatography eluting with 50% *v/v* CH₂Cl₂/hexane switching to 70% CH₂Cl₂/hexane. Removal of solvent under reduced pressure gave product as a yellow solid (150 mg, 55% yield). Crystals suitable for X-ray diffraction were obtained by layering with CH₂Cl₂/*n*-hexane.

¹H NMR (400 MHz, CDCl₃) δ 8.10 (s, 2H), 7.71 (s, 2H), 7.02 – 6.92 (m, 4H), 6.87 – 6.75 (m, 8H), 6.08 – 5.98 (m, 4H), 3.45 (hept, *J* = 6.9 Hz, 2H), 1.18 (d, *J* = 6.9 Hz, 12H), ¹³C{¹H} NMR (151 MHz, CDCl₃) δ 153.1, 143.8, 142.7, 138.3, 130.9, 127.1, 127.0, 126.1, 123.1, 123.0, 119.6, 115.3, 28.7, 23.6; HRMS-ASAP-TOF⁺ *m/z* calculated for C₄₂H₃₄N₂O₂S₃ [M]⁺ 694.1782, found: 694.1770; Anal. Calc. for C₄₂H₃₄N₂O₂S₃ Calc with 2 wt.% CH₂Cl₂, 71.42; H, 4.88; N, 3.94 Found: C, 71.64; H, 5.02; N, 3.80; m.p decomp. > 350 °C.

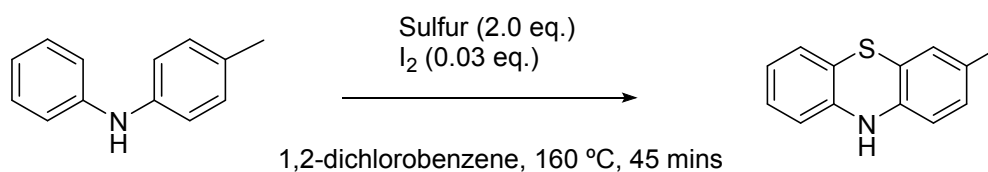
2,8-Bis(1-methylphenothiazin-10-yl)-3,7-diisopropyldibenzothiophene-*S,S*-dioxide
(8)



2,8-dibromo-3,7-diisopropyldibenzothiophene-*S,S*-dioxide (200 mg, 0.44 mmol, 1 eq.) and 1-methylphenothiazine (186 mg, 0.873 mmol, 2 eq.) were dried under vacuum for 30 min in a two-neck 100 mL round-bottomed flask fitted with a reflux condenser. The flask was back-filled with argon and dry toluene (10 mL) was added *via* syringe. The reaction mixture was bubbled with argon for 30 min, then $\text{Pd}_2(\text{dba})_3 \cdot \text{CHCl}_3$ (23 mg, 22 μmol , 0.05 eq.) and $\text{HP}^t\text{Bu}_3\text{BF}_4$ (13 mg, 45 μmol , 0.1 eq.) was added and the reaction mixture was bubbled with argon for a further 30 min. NaO^tBu (126 mg, 1.31 mmol, 3 eq.) was added under a high flow of argon and the reaction was then heated to 107 °C with stirring for 18 h. At the end of the reaction the solvent was removed under reduced pressure and the crude mixture was purified by silica gel column chromatography eluting with 40–70% CH_2Cl_2 /hexane (*v/v*) in 10% increasing increments. Removal of solvent under reduced pressure gave a yellow powder, which was suspended in ethanol and boiled while toluene was added dropwise. Little dissolution was observed and the mixture was hot filtered giving a purer filtrand (**NOT** filtrate). This filtrand was purified by silica gel column chromatography eluting with 40% *v/v* CH_2Cl_2 /hexane to give a yellow solid (60 mg, 19% yield). Crystals suitable for X-ray analysis were obtained by layering of either CH_3CN or butan-1-ol on top of a solution of **8** in CDCl_3 .

^1H NMR (400 MHz, CDCl_3) δ 8.19 (s, 2H), 7.81 (s, 2H), 7.45 (dd, $J = 8.3, 1.2$ Hz, 2H), 7.22 (dd, $J = 7.6, 1.6$ Hz, 2H), 7.18 – 7.10 (m, 4H), 7.04 (td, $J = 7.6, 1.2$ Hz, 2H), 7.00 (t, $J = 7.6$ Hz, 2H), 6.95 – 6.90 (m, 2H), 4.09 (apr. p, $J = 6.8$ Hz, 2H), 1.98 (s, 6H), 1.03 (d, $J = 6.8$ Hz, 12H), $^{13}\text{C}\{^1\text{H}\}$ NMR (176 MHz, CDCl_3) δ 151.0, 149.3, 144.7, 143.1, 136.3, 132.1, 131.3, 131.1, 129.3, 129.1, 127.9, 127.3, 125.9, 125.7, 125.5, 125.0, 122.0, 121.5, 28.8, 23.9, 21.7; HRMS-ASAP-TOF⁺ m/z calculated for $\text{C}_{44}\text{H}_{39}\text{N}_2\text{O}_2\text{S}_3$ $[\text{MH}]^+$ 723.2174, found: 723.2173, Anal. Calc. for $\text{C}_{44}\text{H}_{38}\text{N}_2\text{O}_2\text{S}_3$, 73.10; H, 5.30; N, 3.87 Found: C, 72.99; H, 5.34; N, 3.80; m.p decomp. > 350 °C.

3-methylphenothiazine

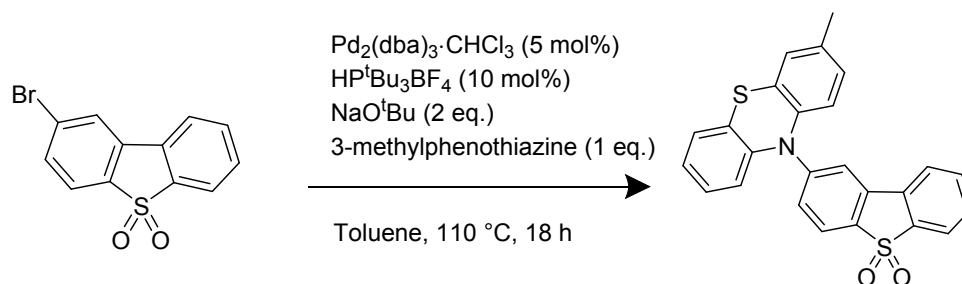


This synthesis was based on a modified literature procedure.^[S23]

To a 50 mL two-neck round-bottomed flask equipped with a stirrer bar and reflux condenser was added *N*-(4-methylphenyl)aniline (2.00 g, 10.9 mmol, 1 eq.). The amine was dried under vacuum for 30 min, and the setup was backfilled with argon. Under a flow of argon was added sulfur (699 mg, 21.8 mmol, 2 eq.) and I₂ (83 mg, 0.327 mmol, 0.03 eq.) and anhydrous 1,2-dichlorobenzene (4 mL). The reaction mixture was then deoxygenated by bubbling with argon for 30 min, and was then heated using a drysyn™ kit set to 160 °C for 45 min. After the reaction mixture cooled to room temperature, saturated sodium thiosulfate_(aq) (10 ml) was added followed by H₂O (20 ml). The reaction mixture was extracted with CH₂Cl₂ (3 × 100 ml). The organic layer was dried with MgSO₄ and was filtered. Removal of solvent under reduced pressure gave crude product. The crude mixture was purified by silica gel column chromatography eluting with CH₂Cl₂:hexane (gradient: pure hexane → 20% CH₂Cl₂:hexane (v/v)). Removal of solvent under reduced pressure gave product as a yellow solid which was recrystallised from hot hexane with slow addition of acetone until dissolution was achieved. Filtration gave high purity product as a yellow crystalline solid (320 mg, 14% yield). Note: The reaction must not be over heated due to loss of a methyl group from the product. Phenothiazine is inseparable from the product here and in subsequent reactions. Note: More product was obtained with approx. 90% purity (650 mg, 28%), however high purity material was imperative for the next step.

Data matches exactly as previously reported in the literature^[S24].

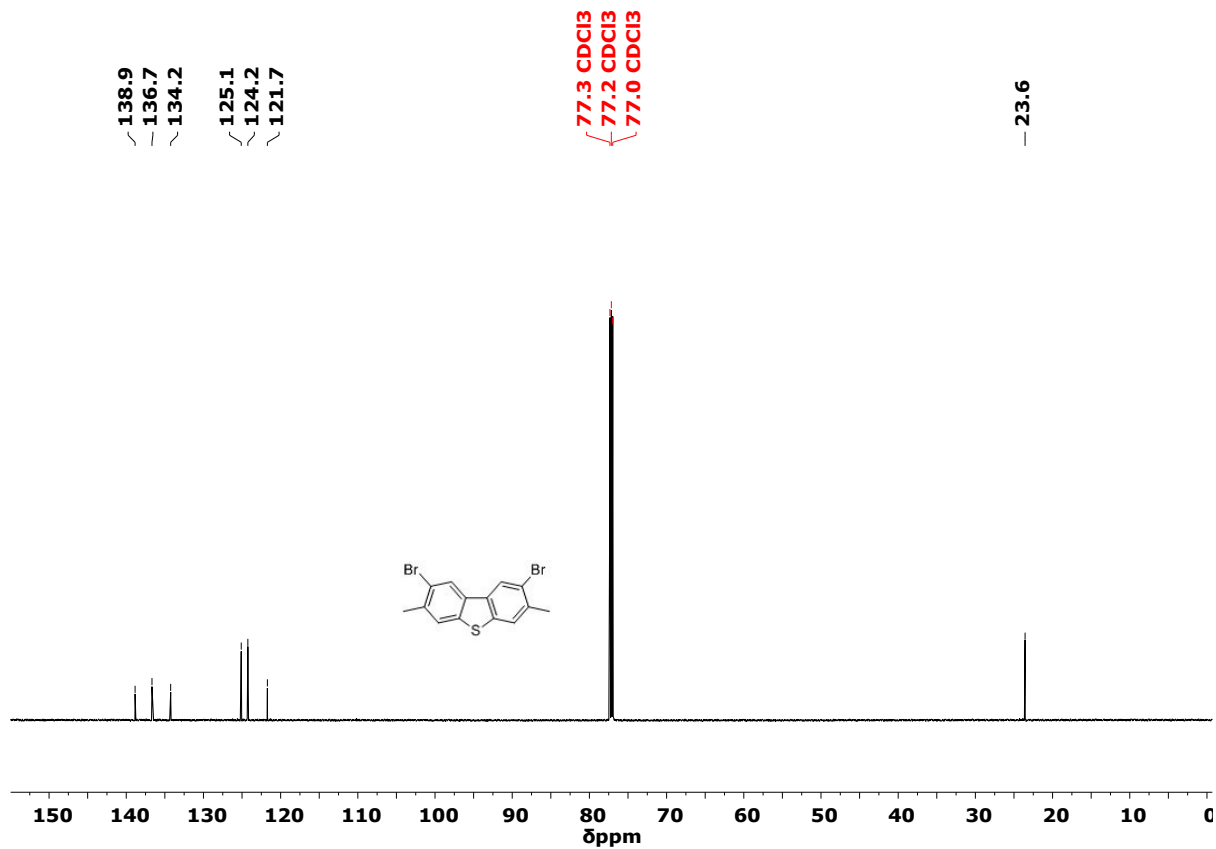
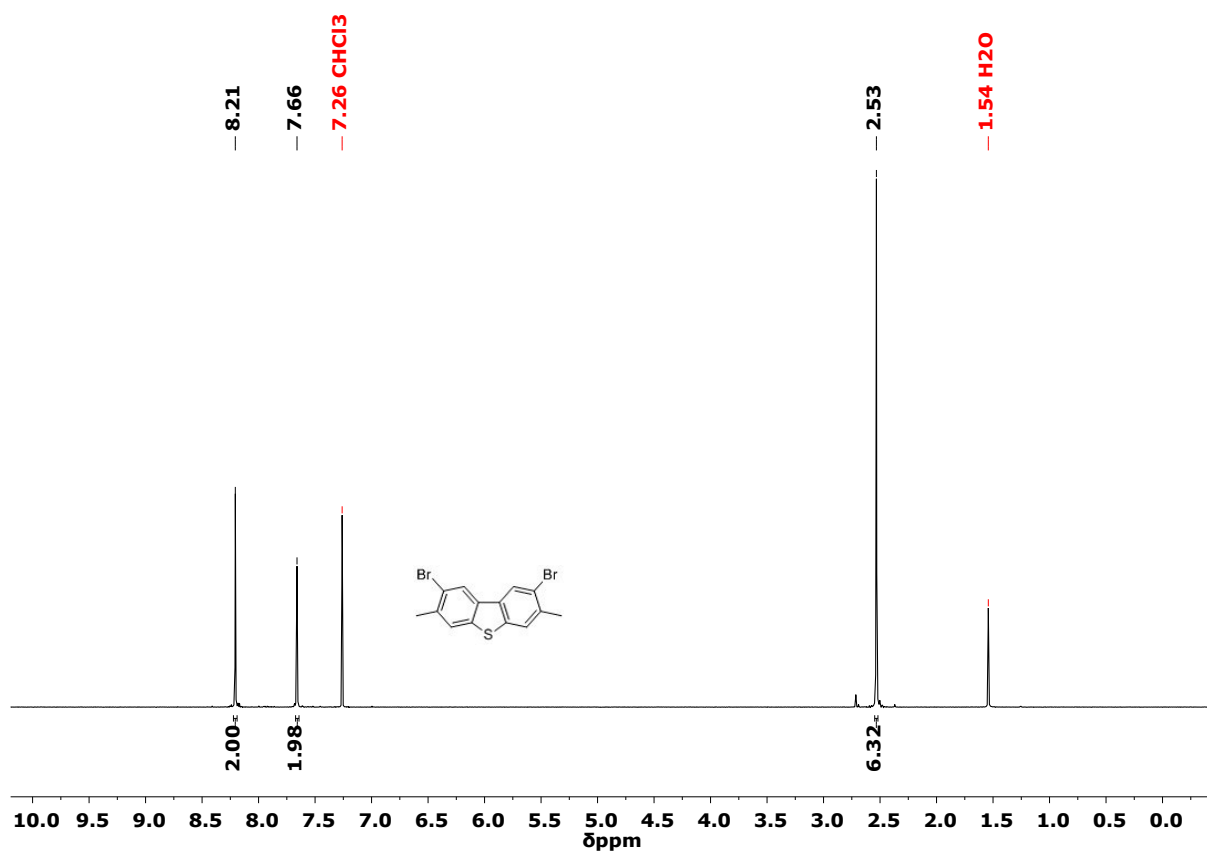
2-(3-methylphenothiazin-10-yl)-dibenzothiophene-*S,S*-dioxide (12)

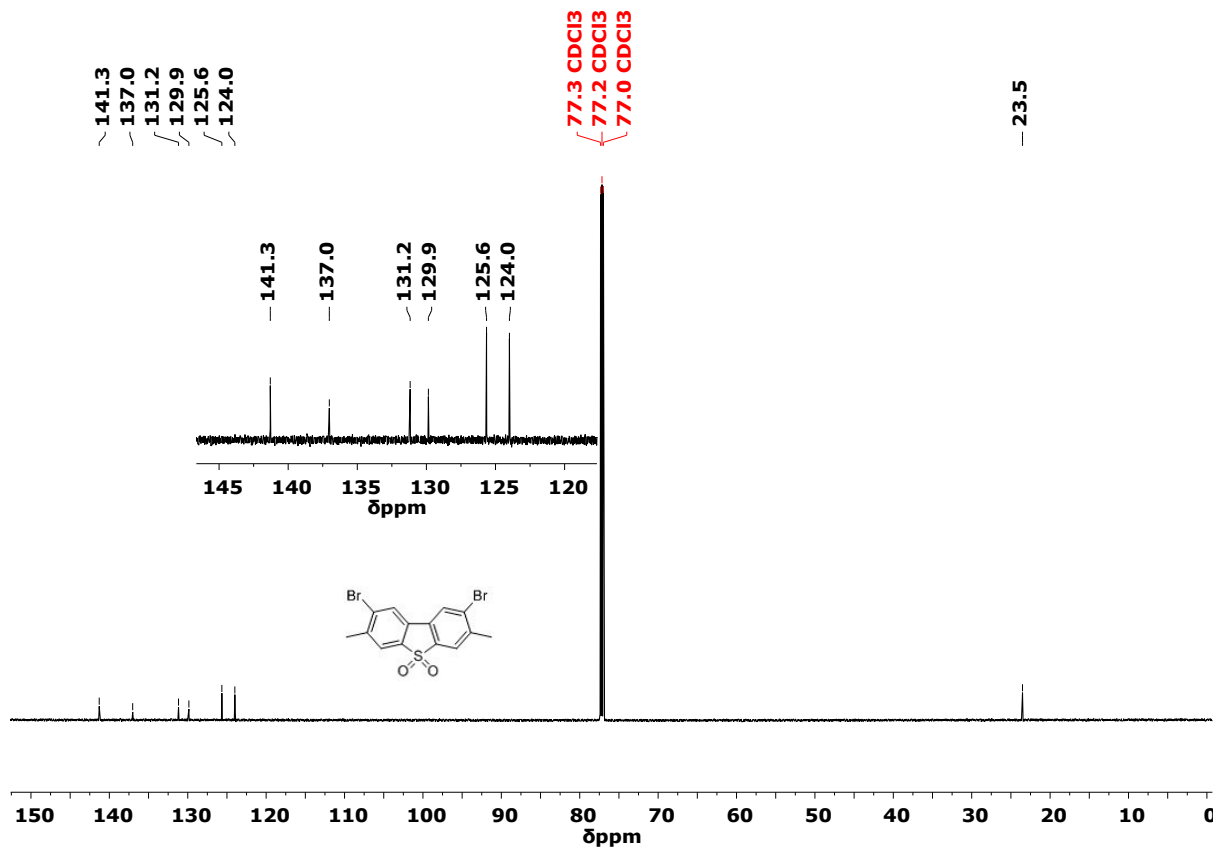
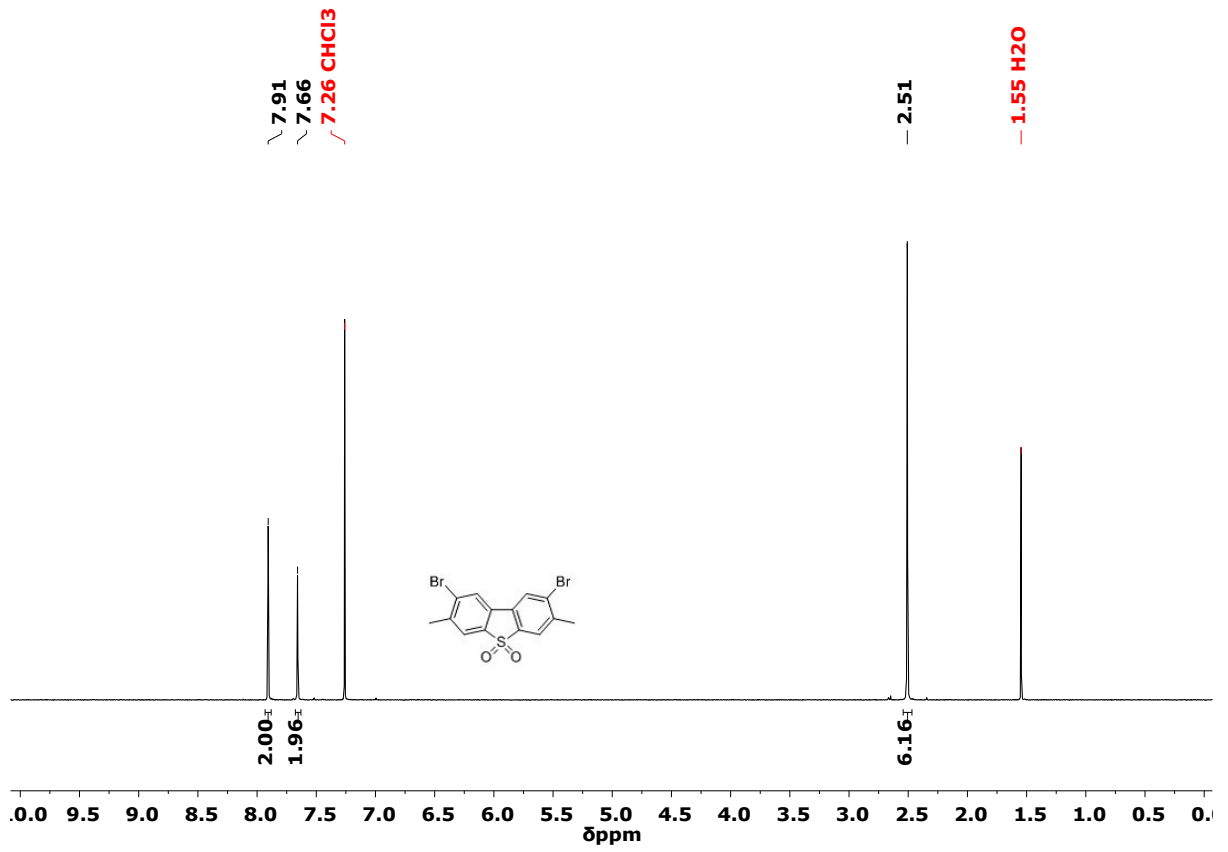


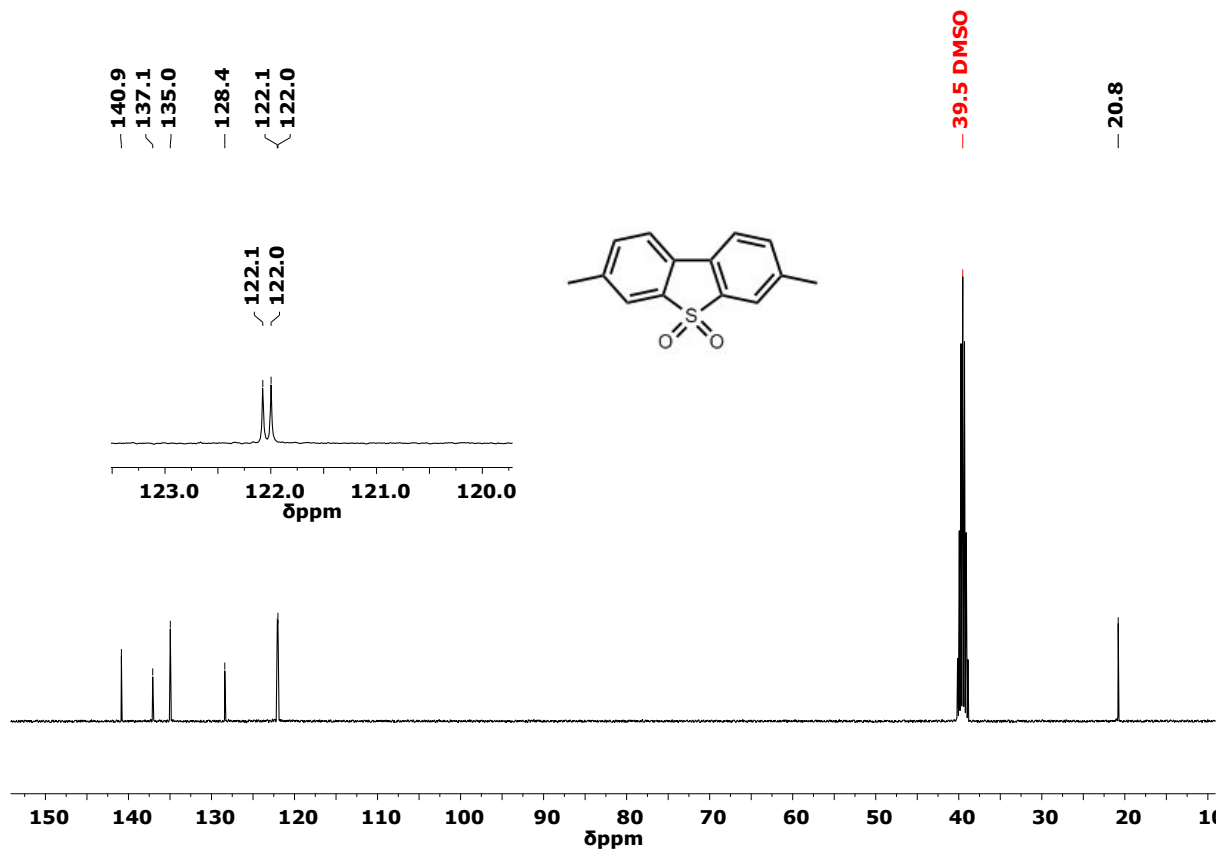
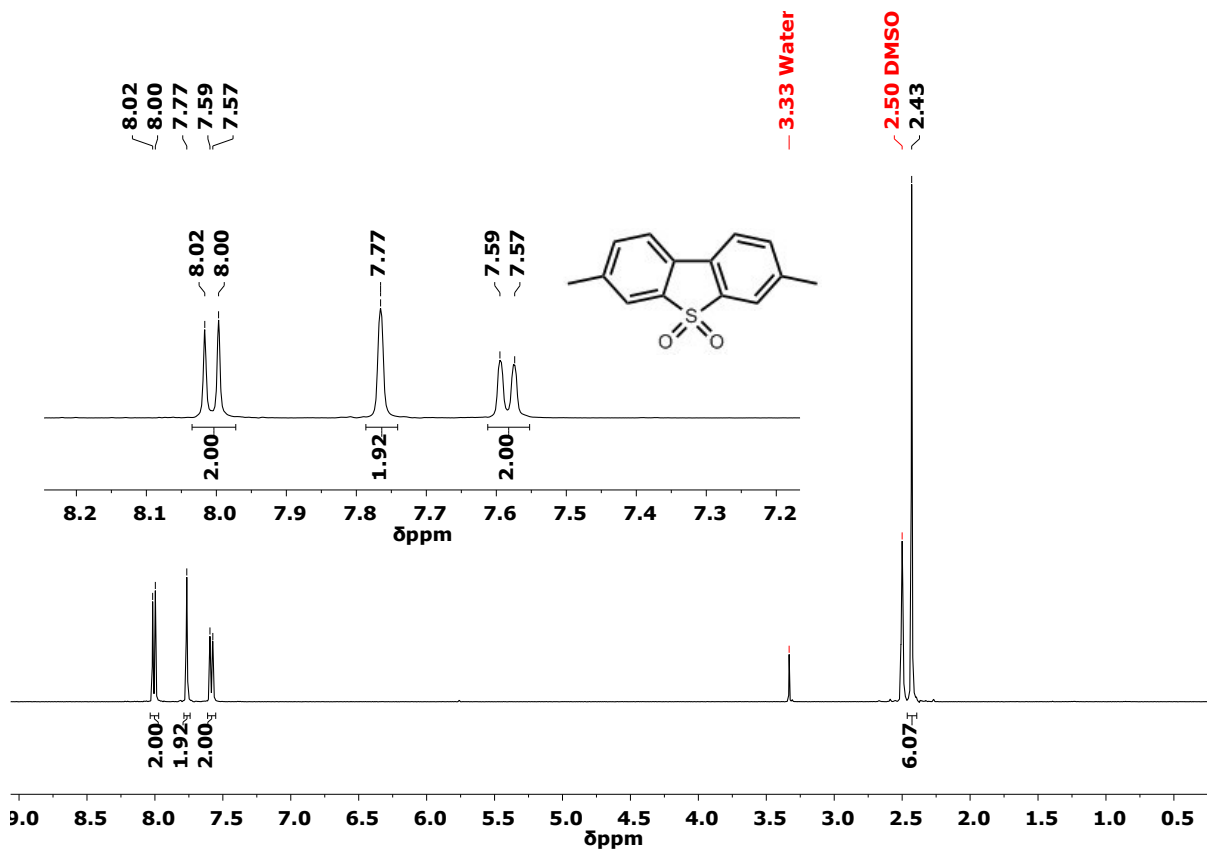
2-Bromodibenzothiophene-*S,S*-dioxide (261 mg, 0.88 mmol, 1 eq.) and 3-methylphenothiazine (189 mg, 0.88 mmol, 1 eq.) were dried under vacuum in a 2-neck 100 mL round bottomed flask equipped with a reflux condenser. The flask was backfilled with argon and anhydrous toluene (15 mL) was added *via* syringe. The solution was deoxygenated by bubbling with argon for 15 min. $\text{Pd}_2(\text{dba})_3 \cdot \text{CHCl}_3$ (46 mg, 44 μmol , 0.05 eq.) and $\text{HP}^t\text{Bu}_3\text{BF}_4$ (26 mg, 0.89 μmol , 0.1 eq.) were added and the solution was bubbled with argon for a further 15 min. NaO^tBu (170 mg, 1.77 mmol, 2.0 eq.) were added and the mixture heated at 110 °C under argon for 18 h. Upon cooling to ambient temperature, water (50 mL) was added and products were extracted into CH_2Cl_2 (3 \times 70 mL). The organic layer was dried over magnesium sulfate and the solvent removed under reduced pressure to give the crude product. The crude product was purified by silica gel column chromatography eluting with CH_2Cl_2 . The solvent was removed under reduced pressure and gave pure product as a yellow solid (120 mg, 32% yield). The product can be sublimed by heating (>210 °C) under high vacuum (5×10^{-2} mbar). Note: Fractions should be analysed individually to obtain product of the best purity. TLC analysis showed column fractions containing only one spot but not all fractions were the same purity. The yield reflects only pure fractions.

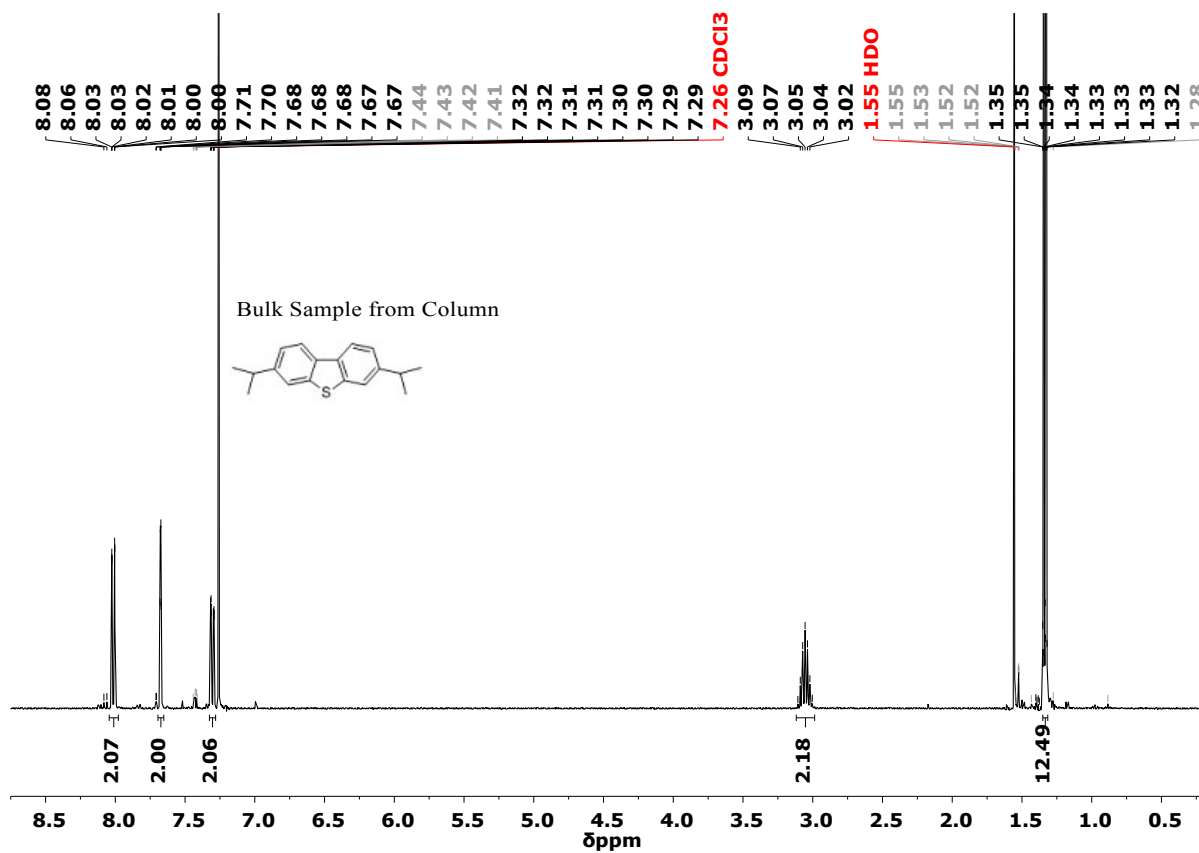
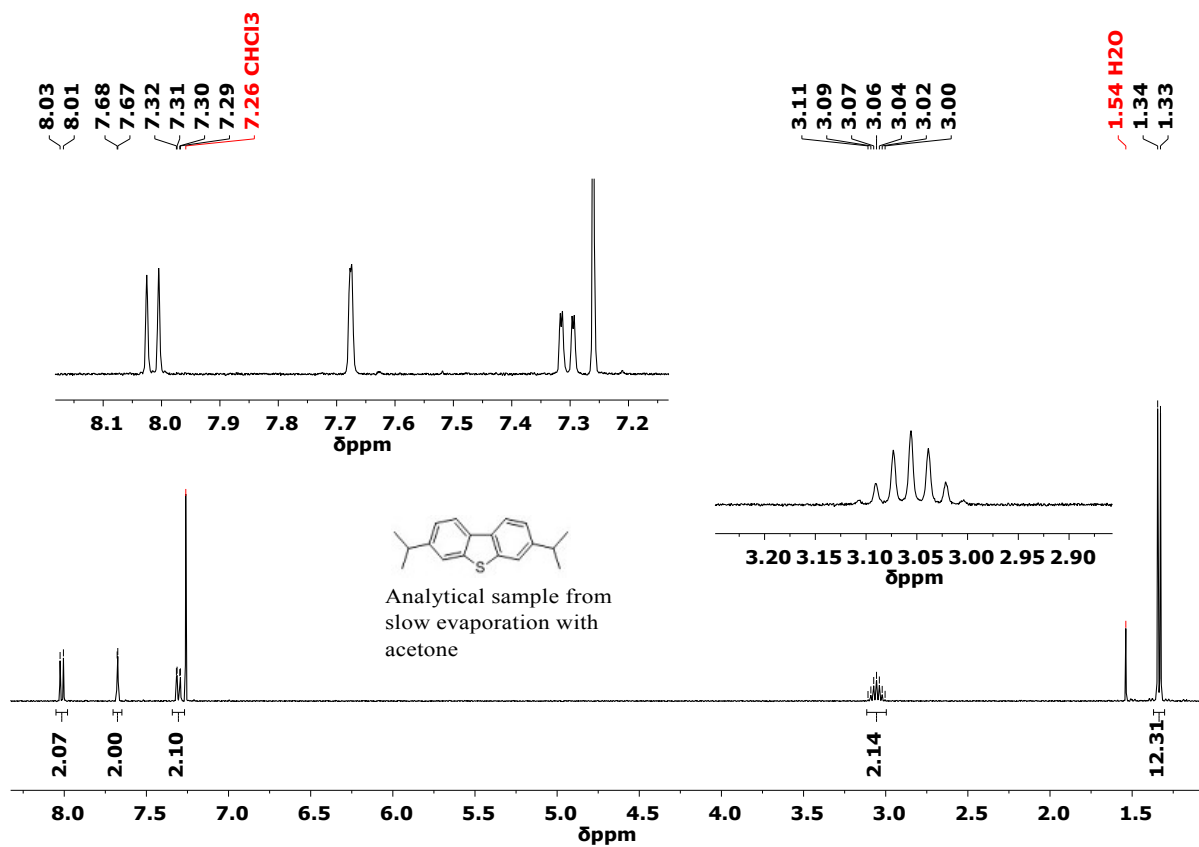
^1H NMR (400 MHz, $\text{DMSO}-d_6$) δ 8.01 (dt, $J = 7.7, 0.9$ Hz, 1H), 7.98 – 7.94 (m, 2H), 7.81 (d, $J = 2.0$ Hz, 1H), 7.75 (td, $J = 7.6, 1.1$ Hz, 1H), 7.65 (td, $J = 7.6, 1.0$ Hz, 1H), 7.43 (dd, $J = 7.7, 1.5$ Hz, 1H), 7.32 – 7.23 (m, 3H), 7.18 (td, $J = 7.5, 1.3$ Hz, 1H), 7.13 – 7.07 (m, 2H), 7.01 (d, $J = 8.2$ Hz, 1H), 2.28 (s, 3H); $^{13}\text{C}\{^1\text{H}\}$ NMR (151 MHz, $\text{DMSO}-d_6$) δ 149.0, 141.4, 138.8, 137.8, 135.0, 134.3, 133.4, 131.3, 131.2, 130.2, 128.4, 128.3, 128.2, 128.1, 127.9, 127.8, 125.4, 124.0, 123.1, 122.9, 122.7, 122.6, 121.8, 113.9, 20.1; HRMS-ASAP-TOF⁺ m/z calculated for $\text{C}_{25}\text{H}_{18}\text{NO}_2\text{S}_2$ $[\text{MH}]^+$ 428.0779, found: 428.0763; Anal. Calc. for $\text{C}_{25}\text{H}_{17}\text{NO}_2\text{S}_2$: C, 70.23; H, 4.01; N, 3.28. Found: C, 70.19; H, 3.99, N, 3.23. m.p 210 – 212 °C.

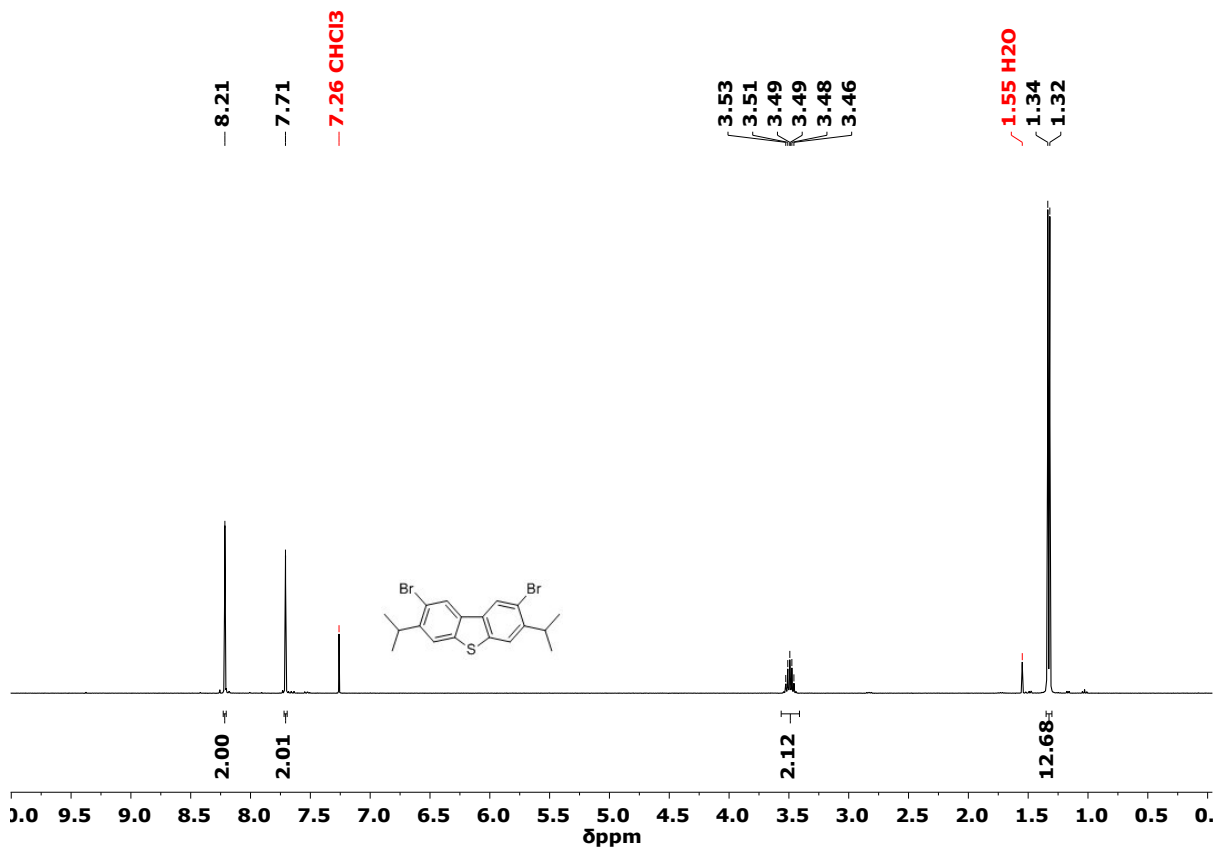
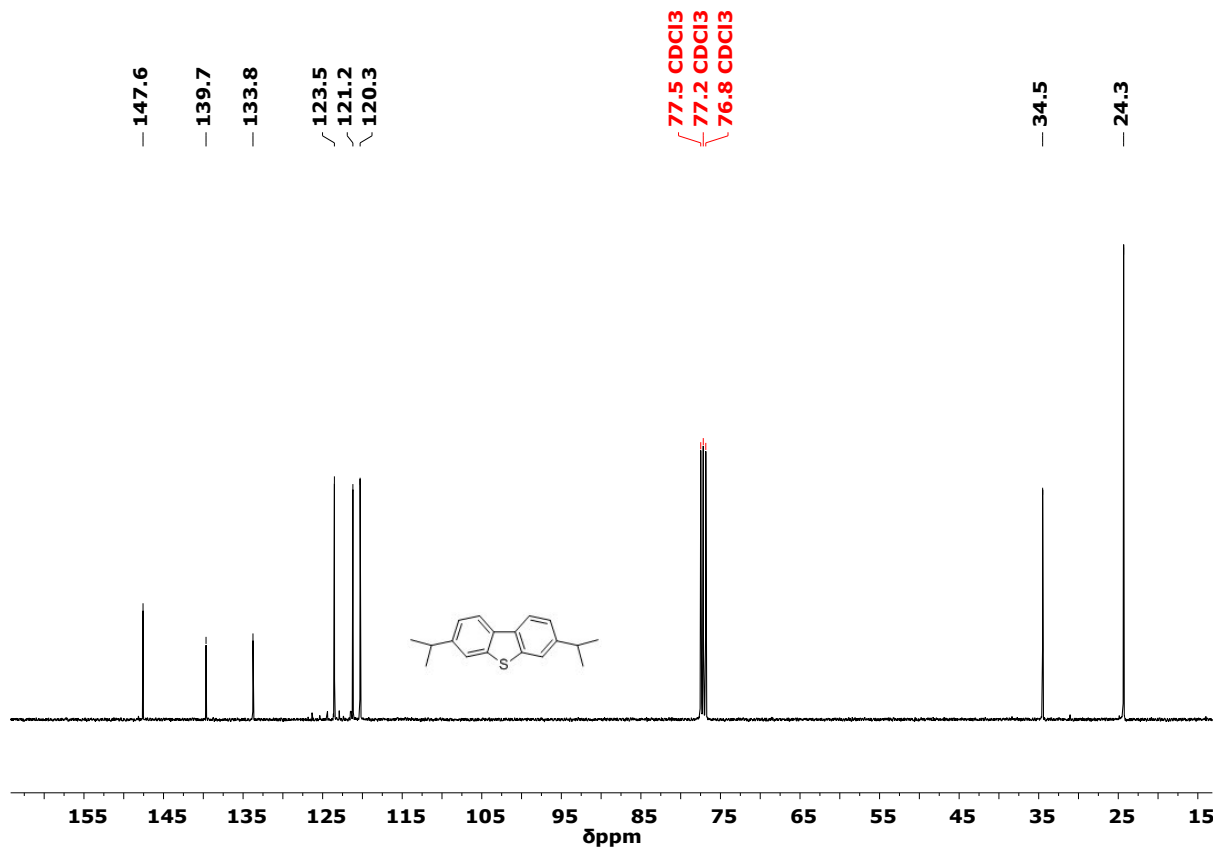
^1H and $^{13}\text{C}\{^1\text{H}\}$ NMR spectra

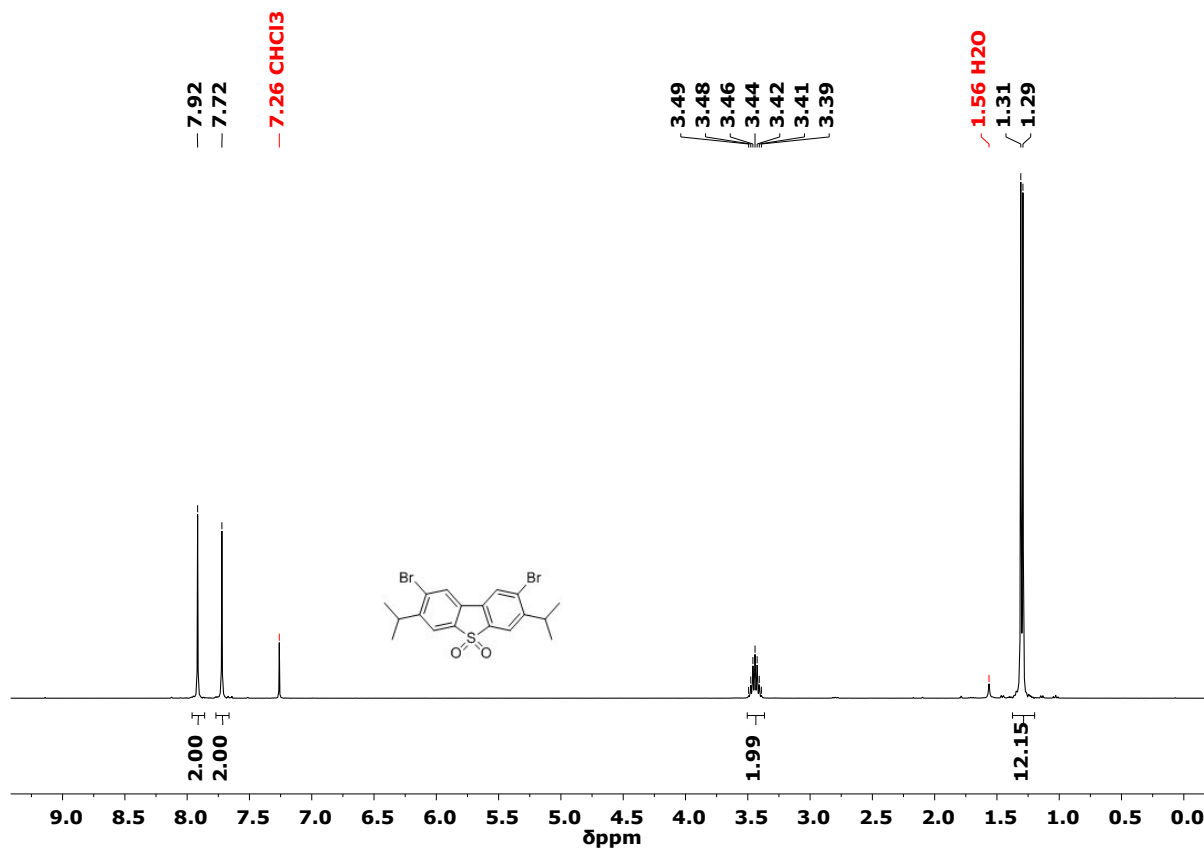
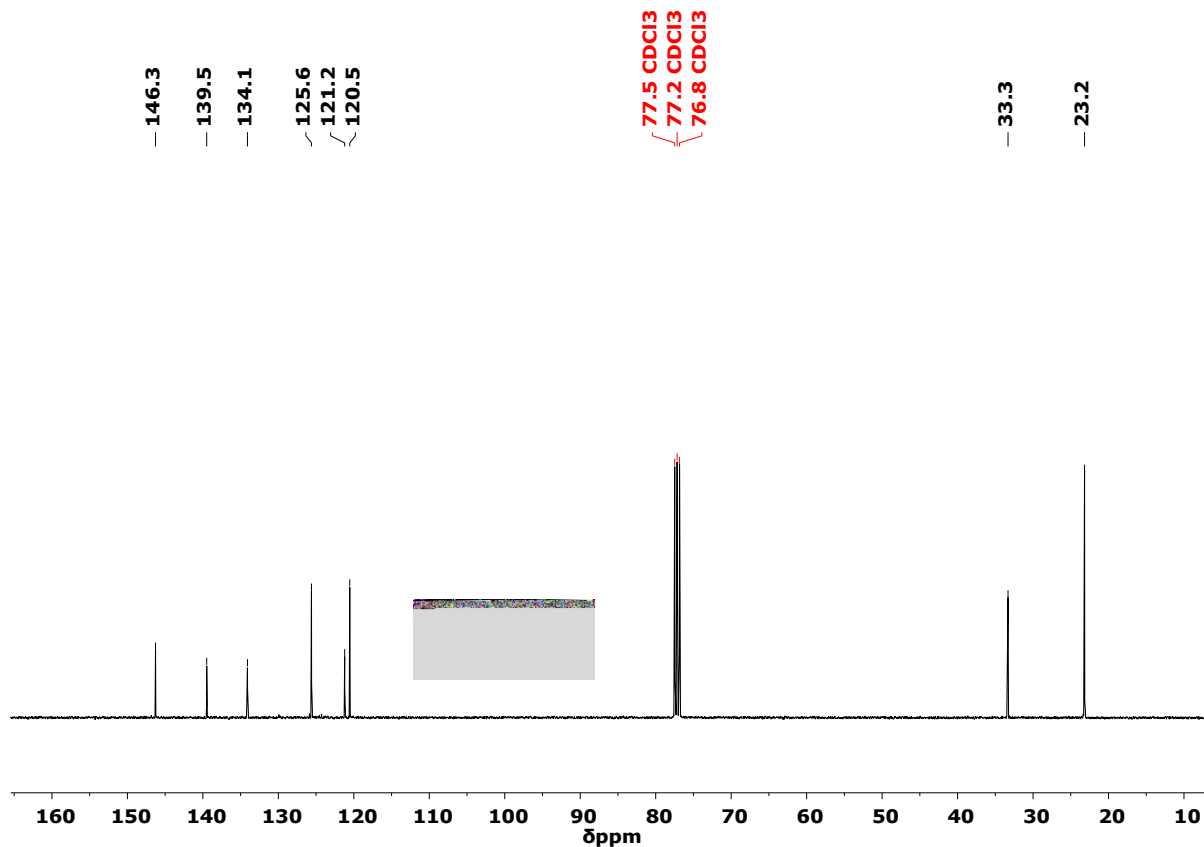


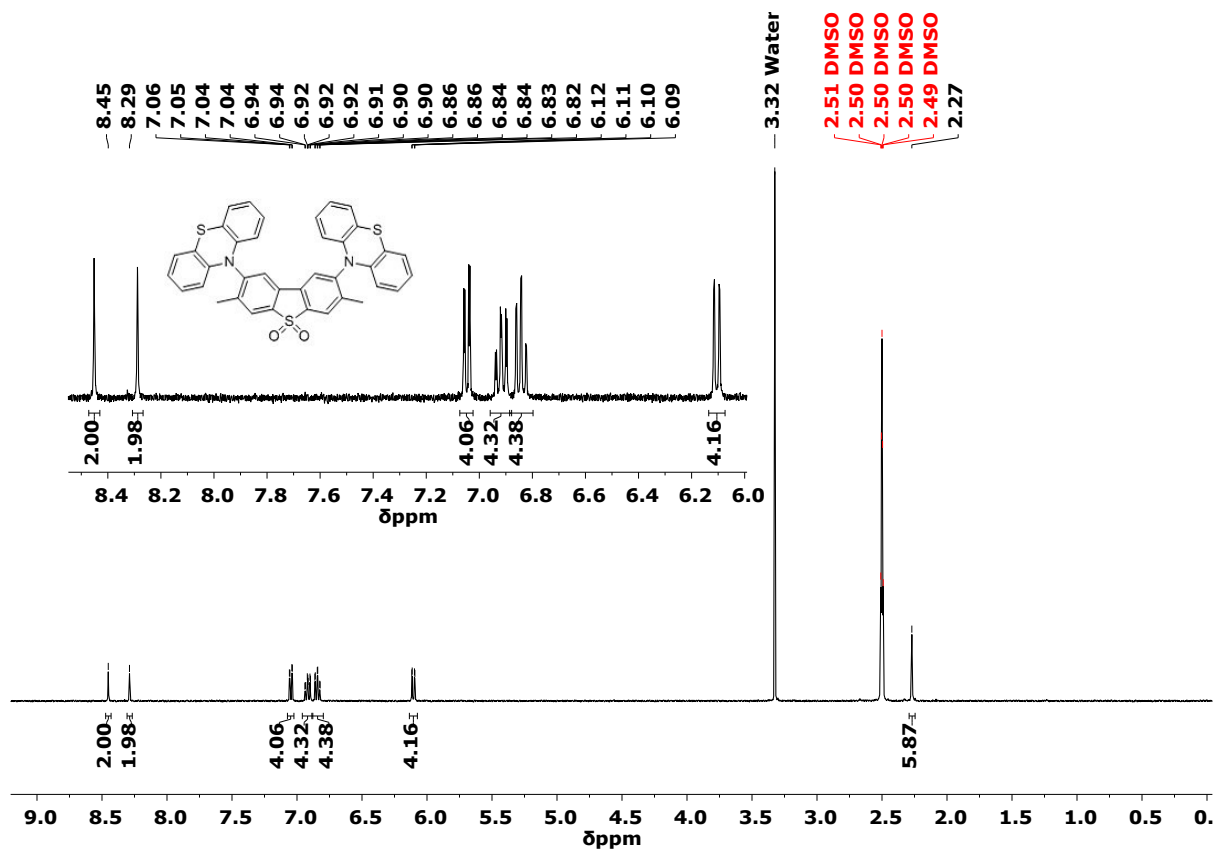
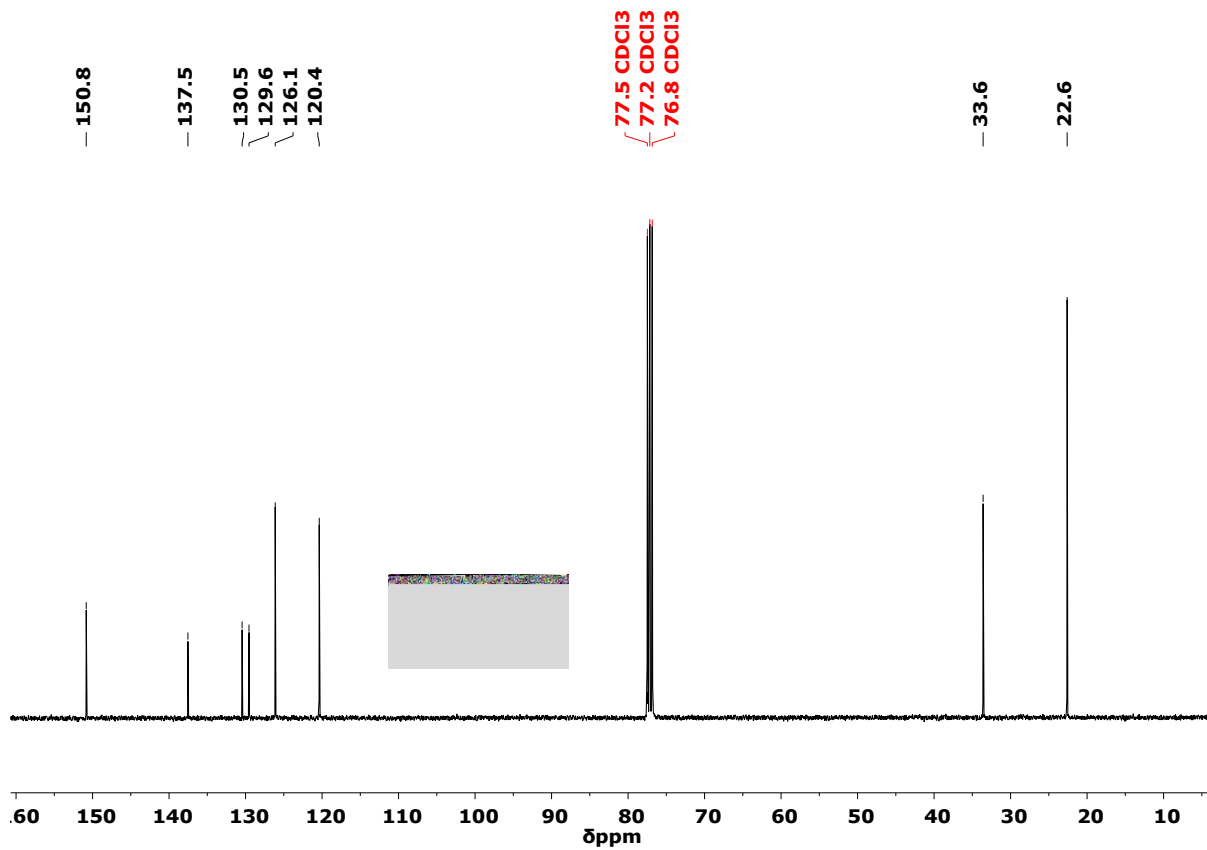


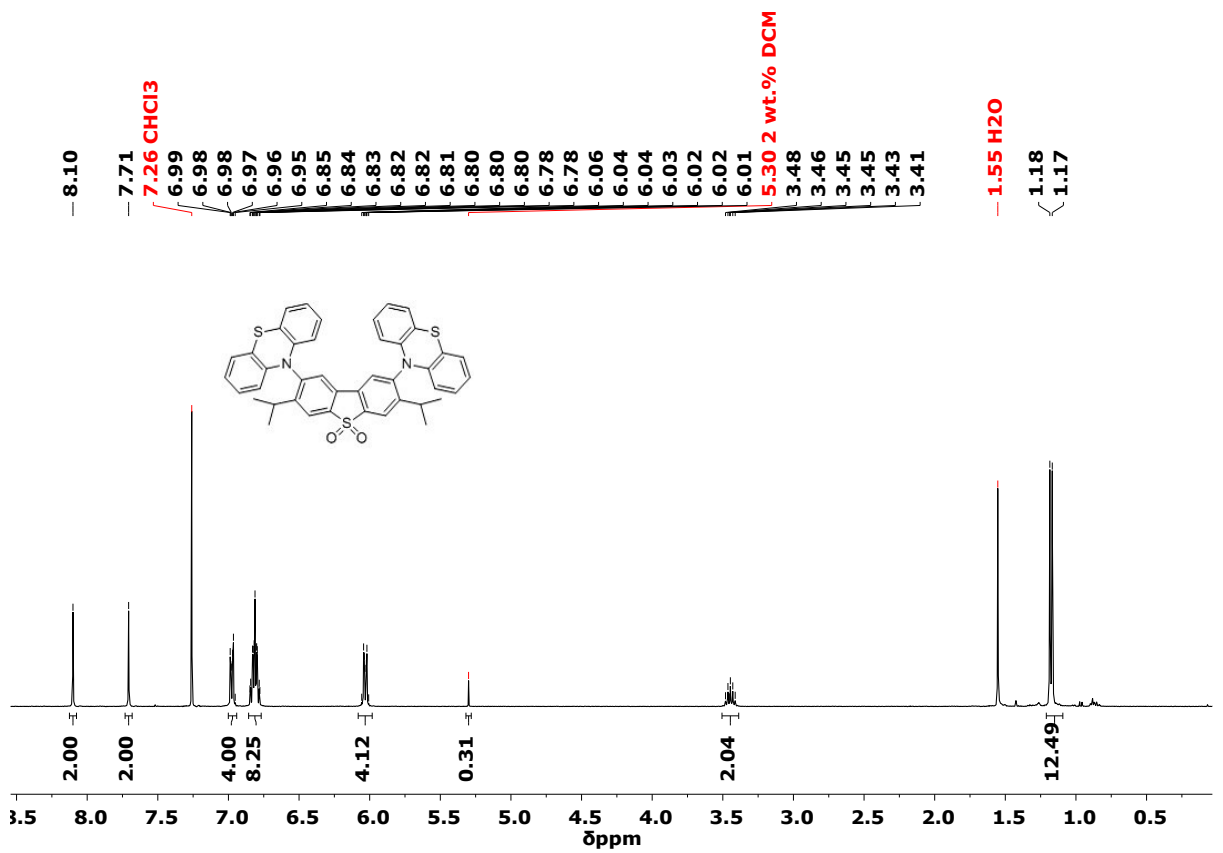
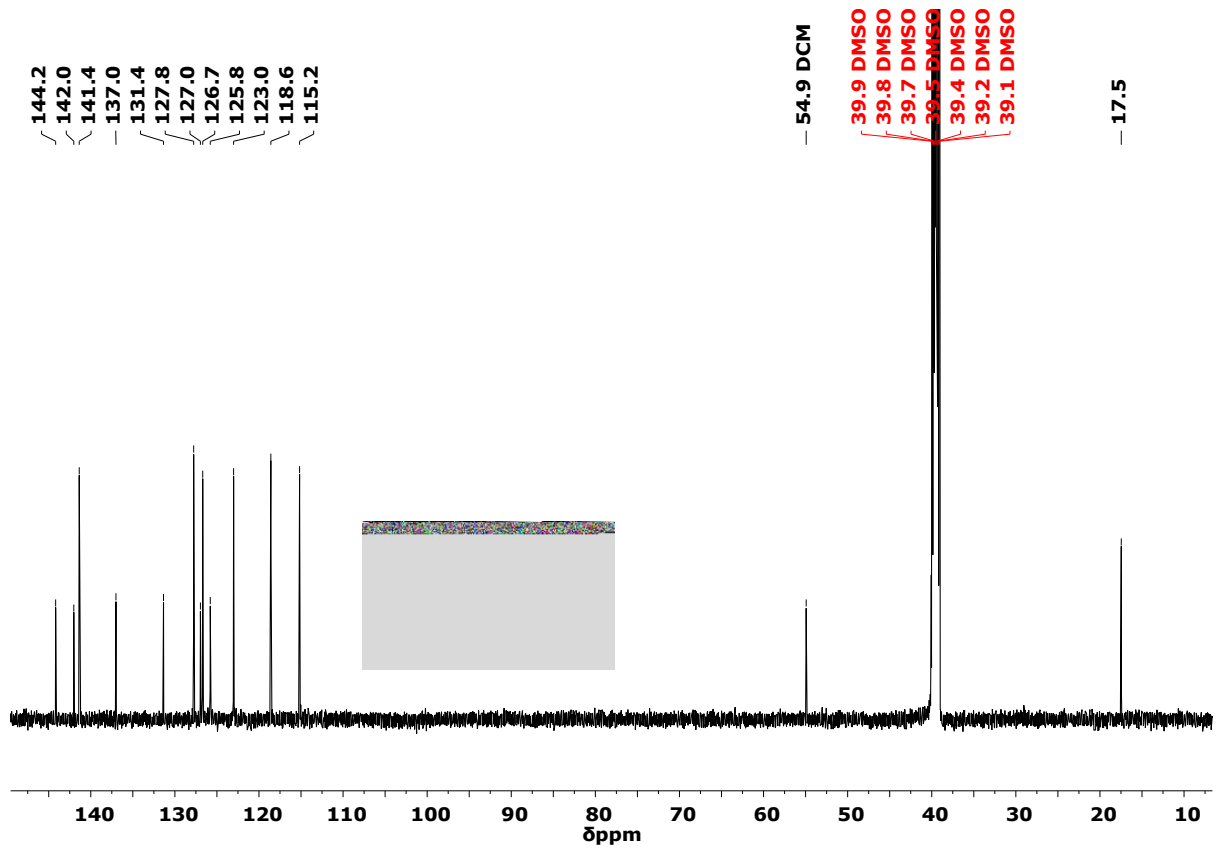


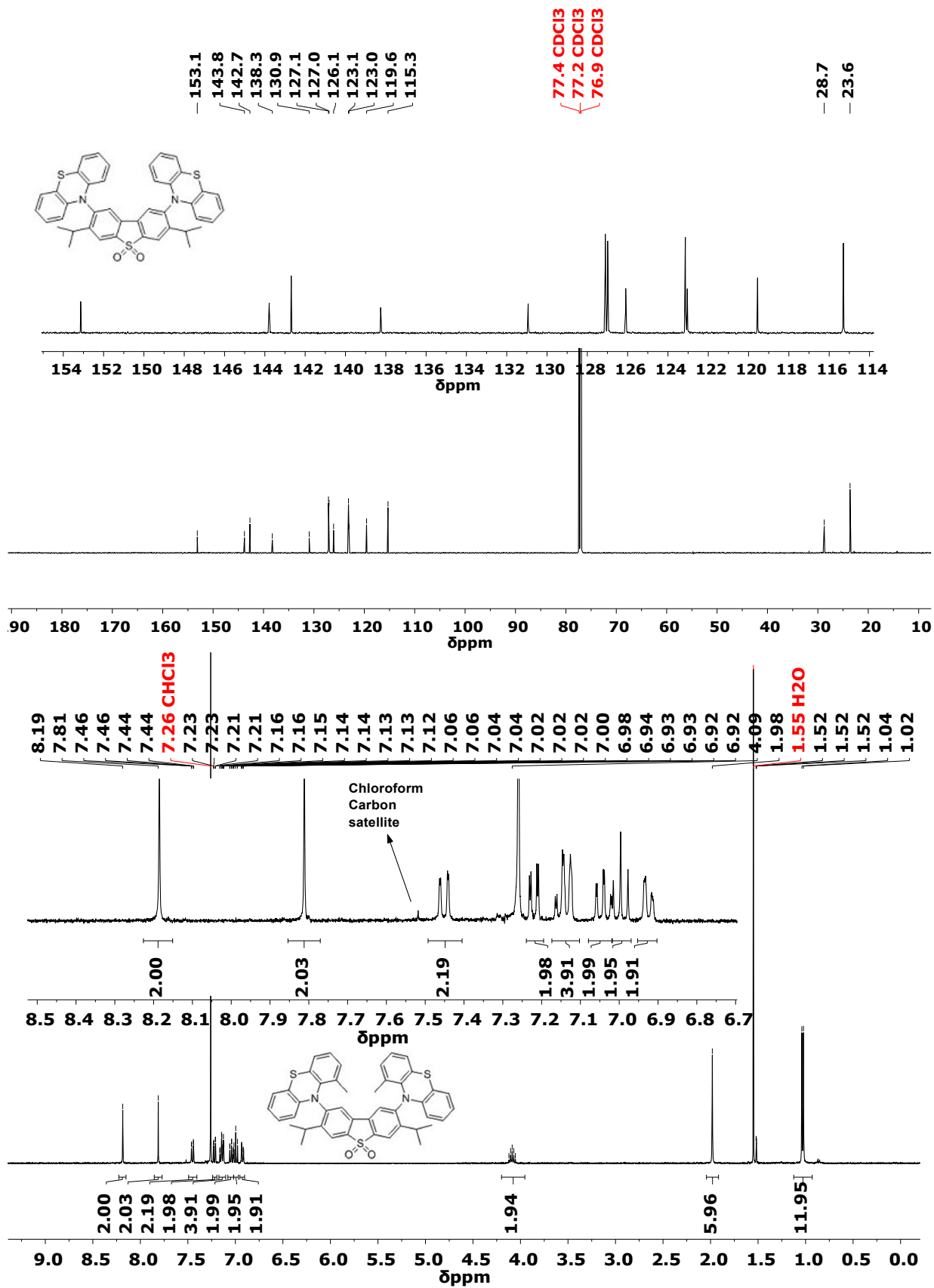


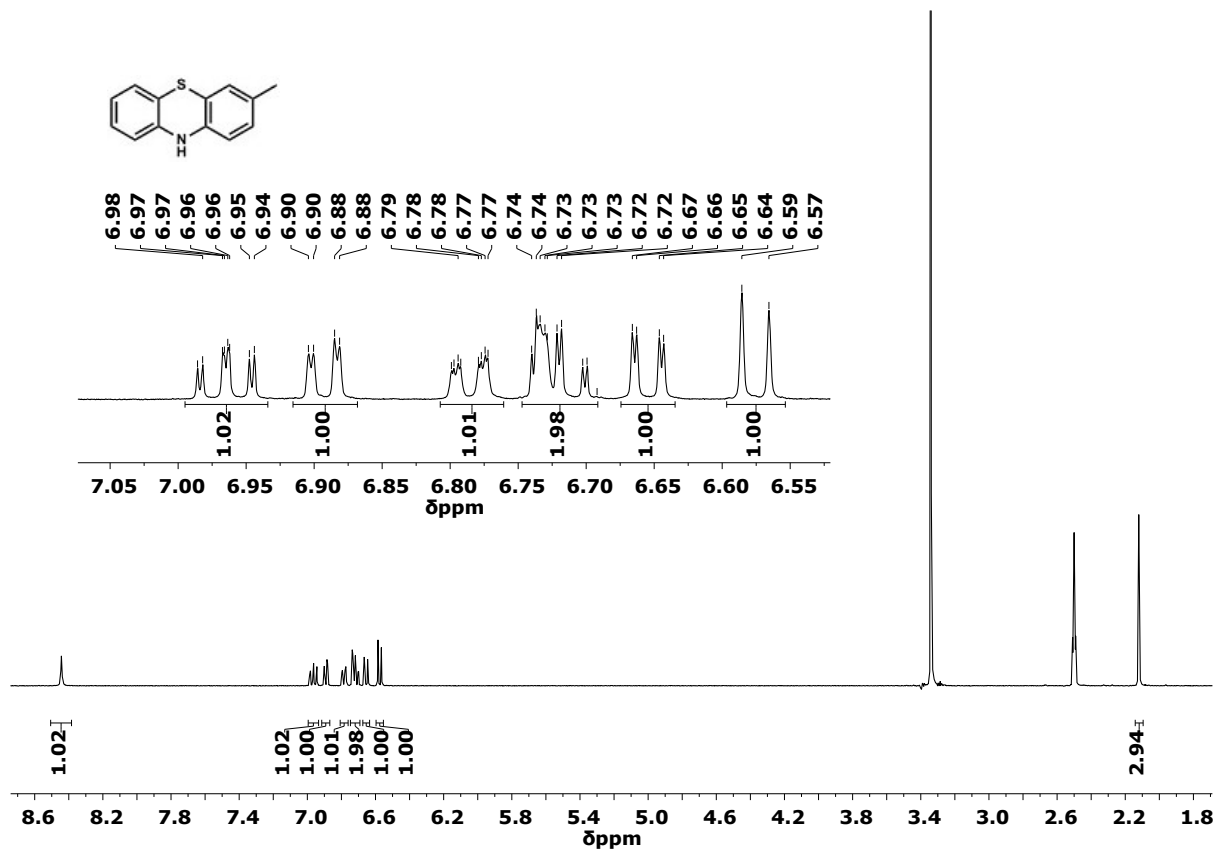
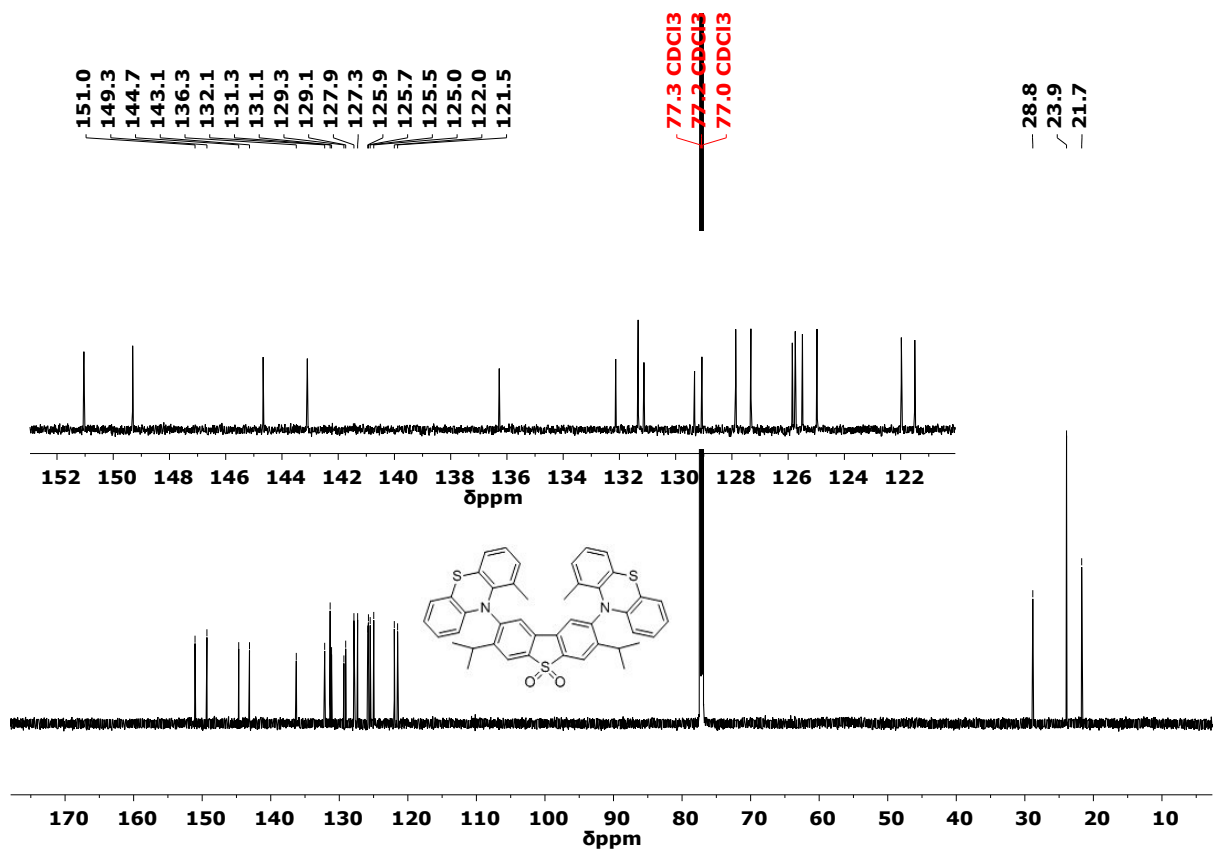


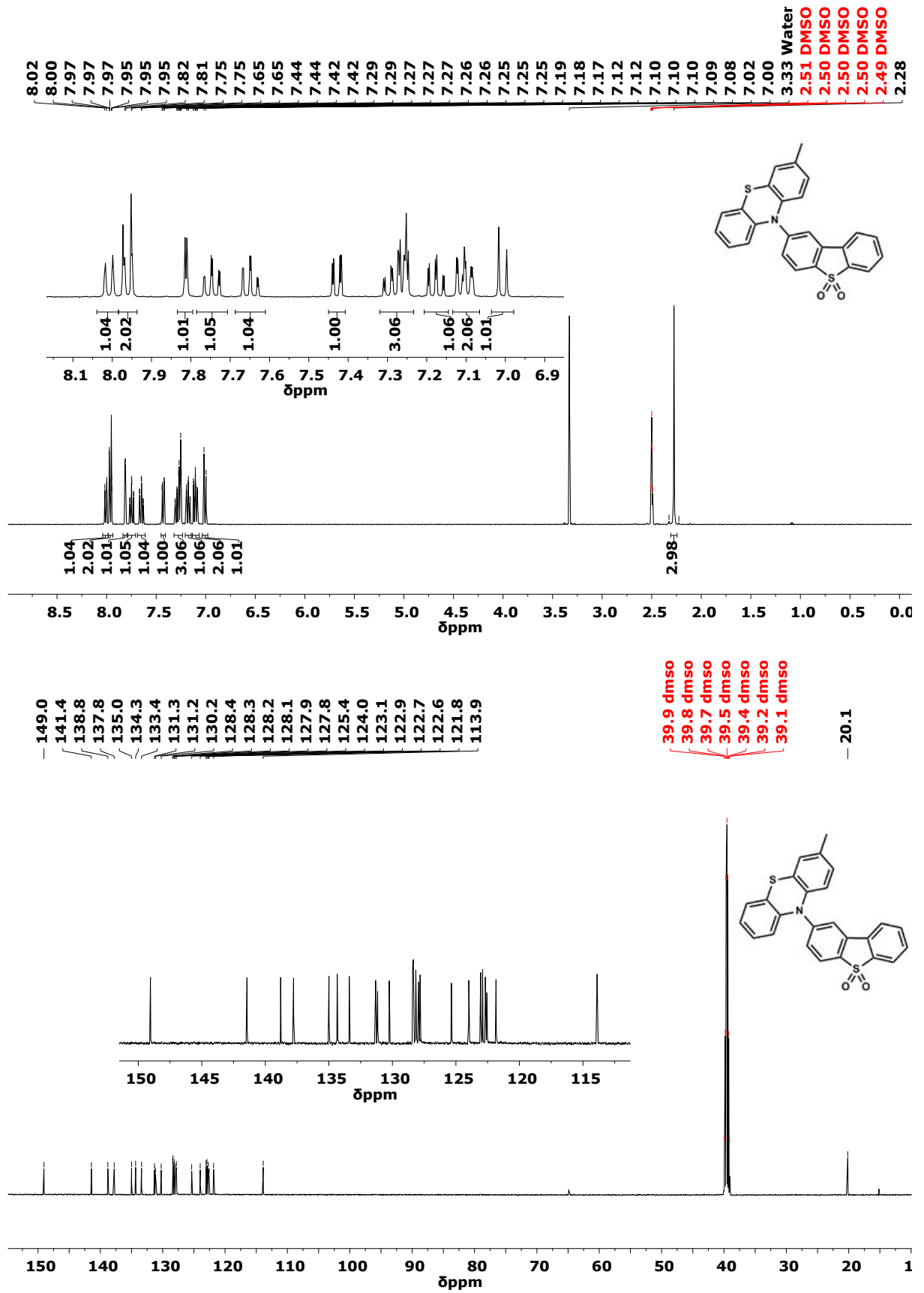












Spectroscopy and photophysics. Thin films in zeonex were prepared by spin coating with guest:zeonex ratio of (1:20 w/w) from toluene solutions. Absorption and emission spectra were collected using a UV-3600 double beam spectrophotometer (Shimadzu), and a Fluorolog fluorescence spectrometer (Jobin Yvon). The extinction coefficient determination was performed in DCM solution. Phosphorescence, prompt fluorescence (PF), and delayed emission (DF) spectra and decays were recorded using nanosecond gated luminescence and lifetime measurements with either a high energy pulsed Nd:YAG laser emitting at 355 nm (EKSPLA) with pulse width \approx 170 ps. Emission was focused onto a spectrograph and detected on a sensitive gated iCCD camera (Stanford Computer Optics) having sub-nanosecond resolution. PF/DF time resolved measurements were performed by exponentially increasing the gate and delay times. In general, time gated acquisition of luminescence signals is performed using increasing delay times, while the integration time is kept constant. The disadvantage in this method is that for weak signals, no luminescence can be measured at long-delay times with good S/N ratio. An alternative to this approach is to use increasing delay and integration times, so weak signals can be measured with good S/N ratio, as the integration time increases with delay time. The delay and integration times are chosen in a way that the next delay is set at a time longer than the previous delay+integration time. Therefore, no spectral overlap exists between the spectra corresponding to successive delays. The curve obtained directly from this process does not represent the real luminescence decay. However, this is easily corrected by integrating the measured spectra and dividing the integral by the corresponding integration time. In this way, each experimental point represents a snap-shot of the number of photons emitted per second at a time $t = \text{delay} + (\text{integration time})/2$. The luminescence decay is then obtained by plotting each experimental point against time, and fitting with sum of exponentials. When required. In this way we are able to collect luminescence decaying over 8 decades in time and in a single experiment.^[S25] For initial development of these methods see previously published literature.^[S26]

References:

- [S1] R. Rybakiewicz, P. Gawrys, D. Tsikritzis, K. Emmanouil, S. Kennou, M. Zagorska, A. Pron, *Electrochim. Acta* 2013, **96**, 13-17.
- [S2] S. Trasatti, *Pure Appl. Chem.* 1986, **58**, 955-966.
- [S3] P. Data, R. Motyka, M. Lapkowski, J. Suwinski, A.P. Monkman, *J. Phys. Chem. C*, **119**, 2015, 20188-20200.
- [S4] J.-L. Bredas, *Mater. Horiz.* 2014, **1**, 17-19.
- [S5] Y. Zhao and D. G. Truhlar, *Theor. Chem. Acc.* 2008, 120, 215–241.
- [S6] F. Weigend and R. Ahlrichs, *Phys. Chem. Chem. Phys.* 2005, **7**, 3297-3305.
- [S7] Gaussian 09, Revision E.01, M. J. Frisch, G. W. Trucks, H. B. Schlegel, G. E. Scuseria, M. A. Robb, J. R. Cheeseman, G. Scalmani, V. Barone, B. Mennucci, G. A.

Petersson, H. Nakatsuji, M. Caricato, X. Li, H. P. Hratchian, A. F. Izmaylov, J. Bloino, G. Zheng, J. L. Sonnenberg, M. Hada, M. Ehara, K. Toyota, R. Fukuda, J. Hasegawa, M. Ishida, T. Nakajima, Y. Honda, O. Kitao, H. Nakai, T. Vreven, J. A. Montgomery, Jr., J. E. Peralta, F. Ogliaro, M. Bearpark, J. J. Heyd, E. Brothers, K. N. Kudin, V. N. Staroverov, R. Kobayashi, J. Normand, K. Raghavachari, A. Rendell, J. C. Burant, S. S. Iyengar, J. Tomasi, M. Cossi, N. Rega, J. M. Millam, M. Klene, J. E. Knox, J. B. Cross, V. Bakken, C. Adamo, J. Jaramillo, R. Gomperts, R. E. Stratmann, O. Yazyev, A. J. Austin, R. Cammi, C. Pomelli, J. W. Ochterski, R. L. Martin, K. Morokuma, V. G. Zakrzewski, G. A. Voth, P. Salvador, J. J. Dannenberg, S. Dapprich, A. D. Daniels, Ö. Farkas, J. B. Foresman, J. V. Ortiz, J. Cioslowski, and D. J. Fox, Gaussian, Inc., Wallingford CT, 2009.

[S8] J. Tomasi, B. Mennucci and R. Cammi, *Chem. Rev.*, 2005, **105**, 2999–3094.

[S9] D. R. Allan, H. Nowell, S. A. Barnett, M. R. Warren, A. Wilcox, J. Christensen, L.K. Saunders, A. Peach, M.T. Hooper, L. Zaja, S. Patel, L. Cahill, R. Marshall, S. Trimnell, A. J. Foster, T. Bates, S. Lay, M. A. Williams, P. V. Hathaway, G. Winter, M. Gerstel, R.W. Wooley, *Crystals*, 2017, **7**, 336.

[S10] N. T. Johnson, P. G. Waddell, W. Clegg, M. R. Probert, *Crystals*, 2017, **7**, 360.

[S11] N. T. Johnson, M. R. Probert, `cbf_to_sfrm.py` (α Version), 2016. https://github.com/nu-xtal-tools/cbf_to_sfrm (accessed 31/1/19)

[S12] L. Krause, R. Herbst-Irmer, G. M. Sheldrick, D. Stalke, *J. Appl. Crystallogr.* 2015, **48**, 3-10.

[S13] L. J. Bourhis, O.V. Dolomanov, R. J. Gildea, J. A. K. Howard, H. Puschmann, *Acta Crystallogr. A*, 2015, **71**, 59-75.

[S14] G. M. Sheldrick, *Acta Crystallogr. A*, 2008, **64**, 112-122.

[S15] G. M. Sheldrick, *Acta Crystallogr. A*, 2015, **71**, 3-8.

[S16] G. M. Sheldrick, *Acta Crystallogr. C*, 2015, **71**, 3-8.

[S17] O. V. Dolomanov, L. J. Bourhis, R. J. Gildea, J. A. K. Howard, H. Puschmann, *J. Appl. Crystallogr.* 2009, **42**, 339–341.

[S18] G. R. Fulmer, A. J. M. Miller, N. H. Sherden, H. E. Gottlieb, A. Nudelman, B. M. Stoltz, J. E. Bercaw and K. I. Goldberg, *Organometallics* 2010, **29**, 2176-2179.

[S19] R. Gerdil and E. A. C. Lucken, *J. Am. Chem. Soc.* 1965, **87**, 213-217.

[S20] J. S. Ward, R. S. Nobuyasu, A. S. Batsanov, P. Data, A. P. Monkman, F. B. Dias and M. R. Bryce, *Chem. Commun.* 2016, **52**, 2612-2615.

[S21] F. B. Dias, J. Santos, D. R. Graves, P. Data, R. S. Nobuyasu, M. A. Fox, A. S. Batsanov, T. Palmeira, M. N. Berberan-Santos, M. R. Bryce and A. P. Monkman, *Adv. Sci.* 2016, **3**, 1600080.

[S22] R. S. Nobuyasu, Z. J. Ren, G. C. Griffiths, A. S. Batsanov, P. Data, S. K. Yan, A. P. Monkman, M. R. Bryce and F. B. Dias, *Adv. Opt. Mater.* 2016, **4**, 597-607.

[S23] M. Lucarini, P. Pedrielli, G. F. Pedulli, L. Valgimigli, D. Gigmes and P. Tordo, *J. Am. Chem. Soc.* 1999, **121**, 11546-11553.

[S24] M. N. Huang, D. T. Huang, X. H. Zhu and Y. Q. Wan, *Eur. J. Org. Chem.* 2015, 4835-4839.

[S25] P. Pander, P. Data and F. B. Dias, *J. Vis. Exp.* 2018, **142**, e56614.

[S26] C. Rothe and A. P. Monkman, *Phys. Rev. B*, 2003, **68**, 075208.